Evolution of limb development in cephalopod mollusks

Oscar A. Tarazona[1,2,*], Davys H. Lopez[1], Leslie A. Slota[2], and Martin J. Cohn[1,2,#]

[1]Department of Molecular Genetics and Microbiology, [2]Department of Biology, UF Genetics Institute, University of Florida, Gainesville, FL 32610 USA.

[#]Corresponding author: mjcohn@ufl.edu

Current addresses: O.A.T.: Department of Genetics, Harvard Medical School, Boston, MA 02115; D.H.L.: Department of Genetics and Development, Columbia University, 3227 Broadway, Quad 9A, MC9891 New York, NY; L.A.S.: Department of Cell Biology, Duke University Medical Center, Box 3709, Durham, NC 27710

Abstract

Cephalopod mollusks evolved numerous anatomical novelties, including arms and tentacles, but little is known about the developmental mechanisms underlying cephalopod limb evolution. Here we show that all three axes of cuttlefish limbs are patterned by the same signaling networks that act in vertebrates and arthropods, although they evolved limbs independently. In cuttlefish limb buds, *Hedgehog* is expressed anteriorly. Posterior transplantation of *Hedgehog*-expressing cells induced mirror-image limb duplications. Bmp and Wnt signals, which establish dorsoventral polarity in vertebrate and arthropod limbs, are similarly polarized in cuttlefish. Inhibition of Bmp2/4 dorsally caused ectopic expression of *Notum,* which marks the ventral sucker field, and ectopic sucker development. Cuttlefish also show proximodistal regionalization of *Hth*, *Exd, Dll*, *Dac*, *Sp8/9*, and *Wnt* expression, which delineates arm and tentacle sucker fields. These results suggest that cephalopod limbs evolved by parallel activation of a genetic program for appendage development that was present in the bilaterian common ancestor.

Introduction

Animal appendages have widely varying morphologies and perform a multitude of functions, including locomotion, feeding, and reproduction (Nielsen, 2012; Ruppert et al., 2004). Limbs evolved on multiple occasions, and the absence of shared ontogenetic or morphological precursors of appendages in many animal lineages is consistent with their independent origins (Minelli, 2003; Pueyo and Couso, 2005; Shubin et al., 1997). This has led to the view that appendages in different clades of Bilateria are non-homologous morphological innovations that arose by convergent evolution (Nielsen, 2012; Ruppert et al., 2004). However, despite more than 500 million years of divergence, the independently evolved limbs of arthropods and vertebrates share developmental genetic similarities (Pueyo and Couso, 2005; Shubin et al., 1997; Tabin et al., 1999).

These discoveries led to debate over whether the genetic program for appendage development evolved in the common ancestor of all bilaterians in the early Cambrian, or whether arthropod and vertebrate appendages have undergone rampant convergence of developmental programs (Minelli, 2000, 2003; Panganiban et al., 1997; Pueyo and Couso, 2005; Shubin et al., 1997; Tabin et al., 1999). A major obstacle to resolving this question is that the evidence of a conserved program derives almost exclusively from Ecdysozoa and Deuterostomia (Pueyo and Couso, 2005; Shubin et al., 1997), and little is known about molecular mechanisms of limb development in Spiralia, the third major

superphylum of Bilateria (Grimmel et al., 2016; Prpic, 2008; Winchell and Jacobs, 2013; Winchell et al., 2010).

Within spiralians, the phylum Mollusca is the largest lineage, displaying a rich diversity of body plans (*Figure 1A*) dating back to the Cambrian explosion (Ruppert et al., 2004; Smith et al., 2011). The evolution of arms and tentacles in cephalopod mollusks contributed to the successful adaptive radiation of these agile marine predators (Kroger et al., 2011; Ruppert et al., 2004). Cephalopod limbs are highly muscular appendages that bear cup-shaped suckers on their ventral sides. Arms are short and have suckers along the entire ventral surface (*Figure 1B and C*), whereas tentacles are longer, retractable appendages with suckers restricted to a distal pad (*Figure 1D and E*). Tentacles are thought to be specialized serial homologs of the arms (Arnold, 1965; Lemaire, 1970; Shigeno et al., 2008) and are present in decapods (squid and cuttlefish) but absent in nautilids and octopods. Limbs likely evolved *de novo* in cephalopods (*Figure 1A*), since no homologous precursor structures have been identified in any other mollusk lineages (Lee et al., 2003; Shigeno et al., 2008). To test the hypothesis that cephalopod limbs evolved by recruitment of an ancient gene regulatory network for appendage development that is conserved across Bilateria, we investigated arm and tentacle development in embryos of the cuttlefish, *Sepia officinalis*.

Results

Development of arms and tentacles in the cuttlefish (*Sepia officinalis*)

Cuttlefishes are decapod cephalopods that have eight arms and two tentacles (*Figure 1B-E; Figure 1- supplementary movies 1 and 2*). Fertilized cuttlefish eggs undergo superficial cleavage, and scanning electron microscopy and optical projection tomography show that most embryonic development is restricted to the animal pole (*Figure 1H and I*). The first sign of limb formation is observed at stage 16, when all ten limb primordia (5 on each side) can be detected as small swellings around the periphery of a flat-shaped embryo, which lies at the top of the large yolk mass (*Figure 1H and M*). Analysis of the mitotic marker phospho-histone H3 (PHH3) at stage 15 revealed localized clusters of PHH3-positive cells in each of the early limb primordia (*Figure 1F and G*), indicating that initiation of limb outgrowth is caused by localized cell proliferation. Discrete limb buds are observed from stage 17 (*Figure 1I and N; Figure 1- supplementary movie 3*). As the embryo begins to rise-up on the animal pole around stage 19, the limb buds start to elongate along the proximodistal axis (*Figure 1J and O; Figure 1- supplementary movie 4*), and by stage 24, the differential length and morphology of arms relative to tentacles is apparent (*Figure 1L; Figure 1- supplementary movie 5)*.

Analysis of sucker development showed that a sucker field primordium initially forms as a narrow proximodistal ridge along the ventral surface of each limb (evident by stage 21; *Figure 1P*). At later stages, the sucker field ridge cleaves superficially, segregating

sucker buds from proximal to distal (*Figure 1Q*). As the arms elongate, the sucker buds are laid down on the entire ventral surface of each arm (*Figure 1L and R*; *Figure 1- figure supplement 1A and C-G*), forming four parallel rows across the anteroposterior axis (*Figure 1C; Figure 1- figure supplement 1A*). In the tentacles, the primordial sucker band is restricted to the distal tip, where sucker buds form in eight rows along the anteroposterior axis of the tentacle sucker pads (*Figure 1D; Figure 1- figure supplement 1B*). The full complement of immature sucker bud rows is present on each limb at hatching, and differentiation of the suckers continues during post-hatch development (*Figure 1- figure supplement 1H and I*).

Molecular analysis of cuttlefish limbs reveals conservation of proximodistal, anteroposterior, and dorsoventral patterning networks

To test the hypothesis that cuttlefish limb development is regulated by the same molecular mechanisms that pattern arthropod and vertebrate limbs, despite their independent evolutionary origins, we cloned and characterized cuttlefish orthologs of genes that pattern the three axes of vertebrate and arthropod limbs, and then analyzed their expression patterns during cuttlefish limb development (*Figure 2* and *Figure 2- figure supplements 1-10*).

Partial sequences of cuttlefish cDNAs (*Sepia officinalis* and *Sepia bandensis*) were isolated by rt-PCR, and preliminary identities were determined by comparison with NCBI sequence databases, including the octopus genome. Molecular phylogenetic reconstructions were then made by maximum likelihood phylogenetic inference using

the best amino acid substitution model for each gene family (see Materials and Methods for details). Tree topologies with well-supported bootstrap values showed the position of each cuttlefish gene within the targeted gene families, which included *Wnt*, *Tcf/Lef*, *Frizzled* (*Fzd*), *Dachsund* (*Dac/Dach*), *Notum*, *Patched* (*Ptc/Ptch*), *Hedgehog* (*Hh*), *Bone morphogenetic protein* (*Bmp*), *Specificity protein* (*Sp*), and the ANTP and TALE homeobox gene families (trees are shown in *Figure 2- figure supplements 1-10* and are described below; gene accession ID numbers and the data set used in the phylogenetic analyses is provided in *Figure 2 - Supplementary file 1*).

Within the Wnt family of cell signaling proteins, we isolated cuttlefish orthologs of *Wnt1*, *Wnt2*, *Wnt5,* and *Wnt7* (*Figure 2-figure supplement 1*). Phylogenetic analysis of cuttlefish transcription factors identified *Tcf3/4*, an ortholog of arthropod *Pangolin* and a pro-ortholog of vertebrate *Tcf3* and *Tcf4* (*Figure 2-figure supplement 2*), *Dac*, a pro-ortholog of vertebrate *Dach1* and *Dach2* (*Figure 2-figure supplement 3*), and *Sp8/9*, a pro-ortholog of vertebrate *Sp8* and *Sp9* (*Figure 2-figure supplement 4*). We also identified numerous homeobox genes, which phylogenetic analyses confirmed to be *Dll*, a pro-ortholog of vertebrate *Dlx* genes, *Exd*, a pro-ortholog of vertebrate *Pbx* genes, *Hth*, a pro-ortholog of vertebrate *Meis1* and *Meis2*, and *Engrailed,* a pro-ortholog of vertebrate *En1* and *En2* (*Figure 2-figure supplement 5*).

In addition, we cloned the Wnt extracellular inhibitors *Notum* and *Sfrp-1/2/5*, and the Wnt co-receptor *Fzd9/10* (*Figure 2-figure supplements 6 and 7*). Cuttlefish possess a *Bmp-2/4* gene that is an ortholog of arthropod *Dpp* and a pro-ortholog of vertebrate

Bmp2 and *Bmp4* (*Figure 2-figure supplement 8*), a *Hh* gene (Grimaldi et al., 2008) that we show to be a pro-ortholog of the vertebrate hedgehog family (*Figure 2-figure supplement 9*), and a gene encoding the Hh receptor *Patched*, a pro-ortholog of vertebrate *Ptch1* and *Ptch2* (*Figure 2-figure supplement 10*). The cuttlefish *Sfrp* ortholog that we identified as *Sfrp1/2/5* was annotated incorrectly in the octopus genome as *Frizzled1* (*Figure 2-Supplementary file 1*). We also found two *Sp8/9* genes in the octopus genome (*Figure 2-Supplementary file 1*), and the cuttlefish *Sp8/9* gene shows clear orthology to only one of the two octopus genes (*Figure 2-figure supplement 4)*, suggesting that the *Sp8/9* gene underwent a duplication in cephalopod mollusks. Therefore, we designate the octopus *Sp8/9* paralogs as *Sp8/9a* and *Sp8/9b,* and the cuttlefish *Sp8/9* gene that we isolated is the ortholog of *Sp8/9a*.

We next investigated the spatial and temporal expression patterns of these genes during cuttlefish limb development. Genes that pattern the proximodistal axis of arthropod and vertebrate limbs (Lecuit and Cohen, 1997; Mercader et al., 1999; Panganiban et al., 1997; Pueyo and Couso, 2005) showed similarly polarized patterns of expression along the proximodistal axis of cuttlefish limb buds, with *Exd* and *Hth* restricted proximally (*Figure 2B, F and G; Figure 3A-E; Figure 3-figure supplement 1A and B;* and *Figure 3-figure* supplement 2A, I and J) and *Dll*, *Dac*, *Sp8/9a*, *Wnt1, Wnt5,* and *Wnt7* restricted distally (*Figure 2C, H-J*; *Figure 3F-I*; *Figure 3-figure supplement 1C-E and L-N;* and *Figure 3-figure supplement 2B, C, G, I, and J*). At stages 20-21, the distal expression boundaries of *Exd* and *Hth* and the proximal expression boundaries of *Dll* and *Sp8/9a* appear to mark the morphological boundary between the proximal

sucker-free and the distal sucker-forming regions (compare right panels in *Figure 2F-H and J* with *Figure 1P*). Indeed, at stages when arms and tentacles begin to develop their distinctive morphologies -- tentacles are longer and have an extensive proximal sucker-free domain -- the *Exd*/*Hth* expression domains were found to extend further distally in tentacles (*Figure 3B,D*) compared to arms (*Figure 3A* and *C*). This distal expansion of the *Exd*/*Hth* expression domain matches the expanded sucker-free region and the distal restriction of suckers in tentacles (*Figure 3E*).

Our finding that the proximodistal axis of cuttlefish limbs shares patterns of molecular regionalization with arthropod and vertebrate limbs led us to examine whether anteroposterior and dorsoventral axis development are also conserved. Posteriorly polarized activation of Hedgehog signaling in arthropod and vertebrate limbs is essential for proper patterning of the anteroposterior axis, and ectopic activation of the Hedgehog pathway induces anterior duplication of posterior structures (Basler and Struhl, 1994; Kojima et al., 1994; Riddle et al., 1993). We analyzed *Hh* expression during cuttlefish limb development at stages 16 to 20 and found that *Hh* expression is also polarized to one side of cuttlefish limb buds. In cuttlefishes, however, *Hh* expression is restricted to the anterior margin of the limb bud, whereas in arthropods and vertebrates, *Hh*/*Shh* is expressed posteriorly (*Figure 2D* and *K;* and *Figure 3-figure supplement 2D*). Consistent with the anterior localization of *Hh*, we detected expression of *Patched,* which serves as a readout of Hedgehog signal transduction, in an anterior-to-posterior gradient (*Figure 2L*). Thus, anteroposteriorly restricted activation of the Hedgehog pathway is a conserved feature of cephalopod, arthropod, and vertebrate limb

development, but the polarity of the signaling center is reversed in cephalopod limbs. By stage 21, the anteriorly restricted *Hh* domain has diminished and a new, central expression domain appears in the location of the brachial nerve primordia *(Figure 3-figure supplement 1F,K).*

We then examined the dorsoventral axis, which is controlled by the antagonistic actions of wg/Wnt and dpp/Bmp signaling in arthropods and vertebrates (Brook and Cohen, 1996; Cygan et al., 1997; Diaz-Benjumea et al., 1994; Jiang and Struhl, 1996; Parr and McMahon, 1995). In arthropods, the Wnt ligand *wg* is expressed ventrally, whereas the *Bmp2/4* ortholog *dpp* is expressed dorsally (Basler and Struhl, 1994; Diaz-Benjumea et al., 1994). Expression and function of the Wnt-Bmp network is conserved, albeit with inverted polarity, in vertebrate limbs; *Wnt7a* is expressed dorsally (Parr and McMahon, 1995) and Bmp signaling activates *Engrailed1* (*En1*) ventrally (Ahn et al., 2001), and these interactions regulate development of dorsal and ventral limb structures (Cygan et al., 1997; Parr and McMahon, 1995). During cuttlefish limb development, *Bmp2/4* and *En* show dorsally polarized expression (*Fig 2E, M,* and *N*; and *Figure 3-figure supplement 2E*). Genes encoding Wnt ligands (*Wnt1*, *Wnt5* and *Wnt7*) and cellular components of canonical Wnt signaling cascade (*Tcf3/4* and *Frz9/10*) are expressed broadly throughout the dorsoventral axis of cuttlefish limb buds (*Figure 3F-I* and *Figure 3-figure supplement 1L-R*; and *Figure 3-figure supplement 2G, I, and J*); however, the secreted Wnt antagonists *Notum* and *Sfrp1/2/5* are expressed dorsally in the limb and interlimb regions (*Figure 3J-M*), with the *Sfrp1/2/5* domain extending deeper into the dorsal limb buds (*Figure 2O; Figure 3M*). This dorsal expression of Wnt antagonists

198 suggests a mechanism for restriction of Wnt signaling to the ventral side of the
199 cephalopod limb buds. Taken together, these results suggest that the genetic pathways
200 active along the proximodistal, anteroposterior, and dorsoventral axes of cephalopod
201 limbs are homologous (specifically, orthologous) to the networks that regulate limb
202 development in arthropods and vertebrates.
203
204 In order to further test this hypothesis, we next performed a series of functional
205 experiments to determine whether polarized expression of these signaling molecules is
206 involved in patterning the anteroposterior and dorsoventral axes of cuttlefish limbs
207 (described below). We developed a method for *ex-ovo* culture of cuttlefish embryos (see
208 Material and Methods) to allow *in vivo* manipulations of genetic pathways in early limb
209 buds.
210
211 **Bmp signaling controls dorsoventral patterning of cuttlefish limbs**
212 A hallmark of dorsoventral polarity is the restriction of sucker buds to the ventral surface
213 of the limb (*Figure 1C, D* and *S*), and this is preceded by ventral expression of *Notum* in
214 the sucker-forming region at stage 21 (*Figure 3N-Q*). We asked whether polarized
215 expression of *Bmp2/4* on the dorsal side of cuttlefish limb buds is required for the
216 specification of dorsal identity. To repress dorsal Bmp activity, we implanted carrier
217 beads loaded with Noggin (Nog), a secreted Bmp inhibitor protein, on the dorsal side of
218 stage 17 limb buds (*Figure 4A*). Implantation of Nog beads on the dorsal side of
219 cuttlefish limb buds resulted in ectopic, dorsal expansion of the *Notum* mRNA domain
220 (n=3/3; control PBS [phosphate buffered saline] beads had no effect on *Notum*

expression [n=3/3]) (*Figure 4G,H*). To determine whether inhibition of dorsal Bmp signaling respecifies dorsal cells to form ventral structures, we repeated the experiment and allowed embryos to develop to stage 26-27. Analysis of limb morphology by scanning electron microscopy revealed the presence of ectopic sucker buds on the dorsal surface of Nog-treated limbs (n=8/12; *Figure 4B*; *Figure 4 - figure supplement 1A* and *B)*. The ectopic dorsal suckers extended around the distal tip of the limb and joined the ventral sucker field. By contrast, in limbs that received control PBS beads dorsally, sucker buds were restricted to ventral surface and terminated at the normal dorsal-ventral boundary at the tip of the limb (n=15/15; *Figure 4C*). Our finding that antagonism of Bmp signaling results in development of ventral structures (sucker buds) on the dorsal side of the limb indicates that dorsal *Bmp2/4* activity is required for the early specification of dorsal identity in cephalopod limb development.

Hedgehog signaling at the anterior margin of cuttlefish limb buds controls anteroposterior patterning of the sucker field

We then investigated whether the mechanism of anteroposterior patterning is conserved between cephalopod and vertebrate/arthropod limbs. To determine whether the anterior expression of *Hh* in cuttlefish limb buds controls anteroposterior patterning, we grafted *Hh*-expressing cells from the thickened funnel epithelium (Tarazona *et al*., 2016) to the posterior side of stage 17 limb buds, which created an ectopic source of Hh opposite the endogenous *Hh* expression domain (*Figure 4D*). We used *Hh*-expressing cells from the funnel, rather than the anterior side of the limb bud, to exclude the possibility of grafted limb cells undergoing self-differentiation. Transplantation of *Hh*-expressing cells

to the posterior side of cuttlefish limb buds resulted in posterior limb duplications (n=7/12; *Figure 4E* and *Figure 4 - figure supplement 1C,D*). Analysis of morphology and gene expression in host limbs approximately 10 days after receiving the graft revealed that the posterior duplications even contained sucker buds, which were marked by *Notum* expression (*Figure 4I* and *J*). By contrast, limbs that received control grafts of stage 24 funnel epithelium that lacks *Hh* expression (Tarazona *et al*., 2016) developed normally (n=8/8; *Figure 4F*).

Although these results suggest that *Hh* is sufficient to re-specify anteroposterior polarity in cuttlefish limbs, we wanted to exclude the possibility that posterior identity was induced by other factors that could be present in the graft. Therefore, we tested whether Hh signaling is necessary for anteroposterior patterning of cephalopod limbs by specifically repressing endogenous Hh signaling. A notable morphological feature of cephalopod limbs is the anteroposterior arrangement of parallel sucker rows on the ventral surface (*Figure 1C, D* and *S*). Based on the results of the transplantation experiments, we reasoned that Hh signaling could regulate the number of sucker rows along the anteroposterior axis of cephalopod limbs, similar to the manner in which Hh specifies digit number along the anteroposterior axis of vertebrate limbs (Lewis et al., 2001; Scherz et al., 2007; Zhu et al., 2008).

Transitory treatment (2 days) of cuttlefish embryos at stage 16, when *Hh* is first expressed on the anterior side of the early limb bud, with the small molecule cyclopamine, an inhibitor of Smoothened that represses Hh signaling (*Figure 4K*),

disrupted the anteroposterior distribution of sucker rows in arms and tentacles. Severity of this phenotype ranged from arms with a reduced number of suckers and sucker rows (n=10/10; *Figure 4N* and *O*) to completely sucker-free tentacles (n=8/10*; Figs. 4L*). Control treatments with vehicle only (DMSO) did not alter the normal anteroposterior pattern of sucker rows (n=8/8; *Figure 4M* and *P*). Finally, to confirm that the phenotype of cyclopamine-treated embryos was not due to failure in brachial nerve differentiation, we examined acetylated tubulin immunofluorescence, which shows that the brachial nerve cords develop in both cyclopamine and DMSO treated embryos (*Figure 4 - figure supplement 1E,F*). These results show that Hh signaling is necessary for proper patterning of the anteroposterior axis in cephalopod limb development.

Discussion

Our finding that the proximodistal, dorsoventral, and anteroposterior axes of cuttlefish limb buds are patterned by the same pathways that regulate arthropod and vertebrate limb development suggests that the independent evolution of limbs in cephalopod mollusks involved recruitment of an ancient genetic program for appendage development. Discovery of this appendage developmental circuit within Spiralia demonstrates its deep conservation across all three branches of Bilateria (i.e., Deuterostomia, Ecdysozoa and Spiralia), suggesting its presence in the common ancestor of all bilaterians (Figure 5). Parallel recruitment of this ancient developmental genetic program may have played a role in the independent evolution of a wide diversity of appendages in many bilaterian lineages (Moczek and Nagy, 2005; Shubin et al., 2009).

The discovery that cephalopod, arthropod, and vertebrate appendages develop using conserved developmental mechanisms does not exclude the possibility that other types of appendages evolved by recruiting a different set of developmental tools (or by utilizing the same tools but in different patterns). Examination of gene expression in lateral parapodial appendages of the polychaete worm *Neanthes,* also a spiralian*,* led to the suggestion that the molecular mechanisms of polychaete appendage development might not be conserved with ecdysozoans and deuterostomes (Winchell and Jacobs, 2013; Winchell et al., 2010). However, given that relatively few genes were examined in *Neanthes* parapodia, it is difficult to conclude whether the reported differences between parapodia and arthropod/vertebrate/cephalopod limbs reflect the unique nature of parapodia or lineage-specific divergences that occurred after recruitment of the core developmental program. A study of a different polychaete, *Platynereis dumerilii,* showed that gene expression is generally conserved in appendages that form during regeneration of caudal trunk segments, although some divergent patterns were observed and these were suggested to reflect taxon-specific differences in appendage morphology (Grimmel et al., 2016). How parapodia fit into the picture of animal appendage evolution will require additional studies of spiralian appendages to increase the diversity of species, types of appendages, and number of genes/pathways interrogated. Nonetheless, our discovery that cephalopod arms and tentacles evolved by parallel recruitment of the same genetic program that orchestrates appendage formation in arthropods and vertebrates suggests that this program was present in the bilaterian common ancestor.

Activation of this ancient developmental program could also underlie the origin of other morphological innovations, including non-locomotory appendages such as beetle horns (Moczek and Nagy, 2005; Moczek et al., 2006) and external genital organs of amniote vertebrates (Cohn, 2011; Gredler et al., 2014). We propose that the genetic program for appendage formation was stabilized in Bilateria, including those lineages that lack limbs, for development of appendage-like structures. This hypothesis implies that the ancestral appendage developmental program was not a latent developmental feature that was redeployed each time that limbs evolved, but rather it might have been a continuously activated network that controlled formation of outgrowths in general.

One of our observations raises the possibility that the gene network that controls appendage formation could be conserved in non-cephalopod mollusks, despite the absence of arms and tentacles in those lineages. During cuttlefish funnel/siphon development, we found asymmetric expression of *Hh* (Tarazona *et al*., 2016) and proximodistally polarized expression of *Wnt5* and *Exd*, which partially mirror their expression patterns during arm and tentacle development (Figure 5-figure supplement 1). If this gene network is found to be active in the developing funnel/siphon of non-cephalopod mollusks, then the funnel/siphon would represent a more primitive site of expression in mollusks, given that evolution of the molluscan funnel/siphon predates the origin of cephalopod limbs (Nielsen, 2012; Ruppert et al., 2004). Further studies of gene expression and function during funnel/siphon development in mollusks will be needed to

335 determine if this clade shows conservation of the appendage development program
336 beyond cephalopod arm and tentacle development.
337
338 Although the bilaterian common ancestor may have used this genetic program to control
339 development of rudimentary outgrowths (e.g., appendages, funnel/siphon, genitalia), it
340 is also possible that it predates the evolution of locomotory and non- locomotory
341 appendages. Studies of cephalic neuroectoderm showed that gene expression patterns
342 controlling the anteroposterior axis of the neuroectoderm mirror the organization of gene
343 expression territories along the proximodistal axis of locomotory appendages, including
344 polarized expression of *Sp8*, *Dll*, *Dac* and *Hth* (Lemons et al., 2010). Similarly, Minelli
345 has suggested that the appendage patterning program could reflect co-option of a more
346 ancient (pre-bilaterian) program for patterning the main body axis and, therefore,
347 bilaterian appendages are simply secondary body axes (Minelli, 2000, 2003).
348
349 Cephalopod arms and tentacles have no direct structural homologs in non-cephalopod
350 mollusks; however, they likely formed from the ventral embryonic foot, a morphological
351 and embryological hallmark of the molluscan bodyplan (Nödl et al., 2016). Therefore,
352 cephalopod arms and tentacles may be considered evolutionary novelties that are
353 derived from a structure that is conserved across Mollusca. This raises the question of
354 whether other foot-derived outgrowths/appendages (e.g., in sea slugs) evolved by co-
355 option of the same developmental program that cephalopods, arthropods, and
356 vertebrates use to build appendages.
357

Although the results presented here suggest that an ancient and conserved developmental genetic program facilitated the origin of cephalopod limbs, they also indicate that fine-scale regulatory changes may have played a role in the diversification of cephalopod limb morphologies. For example, evolution of specialized tentacles from serially homologous arms may have resulted from a distal shift in the expression of proximal identity genes, such as *Exd* and *Hth,* which could have extended the proximal sucker-free domain and restricted suckers to a distal pad (*see Figure 3A-E*). Likewise, the results of functional manipulations of Hh signaling in cuttlefish limbs suggests that the diversity in the number of sucker rows in cephalopod limbs (i.e. four rows in squids and cuttlefishes, two in octopus, and one in vampire squid and glass octopus) could be explained by modulation of Hh signaling, in the same way that gradual changes to *Shh* regulation has led to variation in digit number in tetrapod vertebrates (Scherz et al., 2007; Shapiro et al., 2003; Zhu et al., 2008).

Finally, we note that while the data presented here point to the existence of a deeply conserved genetic program for appendage development across *Bilateria*, this does not imply that the limbs of cephalopods, arthropods, and vertebrates are homologous structures, or that limbs were present in the common ancestor. Rather, these results show that homologous developmental mechanisms underlie the multiple parallel origins of limbs in bilaterians.

Materials and Methods

No statistical methods were used to predetermine sample size. Embryos were randomized in each experiment. The investigators were not blinded to allocation during experiments and outcome assessment.

Embryo collection and preparation

Sepia officinalis and *Sepia bandensis* eggs were purchased from commercial suppliers, incubated until they reached the required stages (Lemaire, 1970), and prepared for *in situ* hybridization (ISH) and immunohistochemistry as described (Tarazona et al., 2016).

Optical projection tomography (OPT)

Three-dimensional reconstructions of gene expression in cuttlefish embryos were performed as previously described (Tarazona et al., 2016).

Scanning electron microscopy

Cuttlefish embryos were fixed in 4% paraformaldehyde in phosphate buffered saline (PBS) overnight at 4^{o}C and were washed with PBS the next day. Embryos were fixed in 1% osmium tetroxide solution in PBS for 30 minutes and then washed three times in PBS, dehydrated through a graded ethanol series, critical point dried, and sputter coated with gold. Embryonic samples were scanned using a Hitachi SU5000 and Hitachi TM3000.

Gene cloning and molecular phylogenetic analysis

RNA extraction from *Sepia officinalis* and *Sepia bandensis* embryos at stages 15–26 was performed using TRIzol reagent (Ambion) following the manufacturer's instructions. cDNA synthesis was performed by an AMV reverse transcriptase (New England Biolabs) following the manufacturer's instructions. PCR amplification was carried out on *Sepia* cDNA pools, amplicons were cloned into TA vectors and sequenced. We then performed multiple sequence alignments (MSA) with ClustalW (PMID: 7984417) using the predicted amino acid sequence of our cuttlefish cDNA fragments, and putative

metazoan orthologous genes downloaded from NCBI RefSeq protein databases (Figure 1-Supplementary file 1). We performed nine MSA for Wnt, Tcf, Sfrp, Notum, Patch, Hh, Bmp, Sp and Homeodomain families. Each of the nine MSA was analyzed by ProtTest (PMID: 15647292), in order to determine the best combination of amino acid substitution model and other free parameters (amino acid site frequency, site heterogeneity and invariant sites), using Akaike information criterion (Figure 1-Supplementary file 1). We applied the best model in RaXML (PMID: 18853362) for each MSA and performed maximum likelihood phylogenetic inference, estimating branch support by bootstrap, and then majority consensus of the trees from all bootstrap partitions was performed to compute the final tree topology. All sequences have been deposited in Genbank under accession numbers MK756067-MK756082 (complete list of entries is provided in Supplementary File 1)

In situ hybridization (ISH) and immunohistochemistry

Whole-mount ISH was performed using digoxigenin- and fluorescein-labeled antisense (or sense control) RNA probes according to protocols described previously (Tarazona et al., 2016). Due to limited availability of embryonic material at relevant early developmental stages, only a limited number of *S. bandensis* embryos were used for ISH. Thus, the majority of ISH were performed in *S. officinalis* embryos using *S. officinalis* antisense RNA probe, however, some ISH were performed in *S. officinalis* embryos using *S. bandensis* antisense RNA probes. We validated the specificity of *S. bandensis* probes in *S. officinalis* embryos by comparing the gene expression domains marked by these probes in embryonic material from both species at stages 20 and 21. This comparison shows that gene expression territories identified by these probes at these stages were indistinguishable between the two species (*Figure 3-figure supplement 2*), consistent with their high level of sequence similarity (Figure 3-supplementary file 1). Excluding the *S. bandensis* ISH mentioned above, all the experiments described in this work were carried out with *S. officinalis* embryos. Proliferating cells were detected by immunolocalization of Histone H3 Serine 10 phosphorylation using an antibody against H3S10p/PHH3 (06-570, EMD Millipore) and

brachial nerve tissue was detected using an antibody against acetylated alpha tubulin (ab24610, Abcam).

Cuttlefish *ex-ovo* embryo culture and embryo manipulations

A protocol for *ex-ovo* cuttlefish embryo culture was established for this study, as a modified version of previous descriptions of *ex-ovo* embryo culture in squid (Arnold, 1990). Briefly, to minimize the problem of bacterial and fungal contamination we started the protocol by taking 10 cuttlefish eggs at the appropriate stage, placing them in a 50ml tube, and washing them with 0.22 µm filtered artificial sea water (FASW) five times. Eggs were then cleaned with a freshly prepared 5% bleach solution (0.25% sodium hypochlorite in FASW) for 5 seconds and immediately washed with FASW five times. The bleaching and washing steps were repeated two to three times. Five additional washes with FASW were carried out before incubating the eggs in 2X antibiotic/antimycotic solution (A5955, Sigma) in FASW for 2 hours at ambient temperature.

Each cuttlefish egg was then transferred to a 50 mm diameter petri dish that was coated with a ~ 5mm layer of 0.5% low melting point agarose (16520050, ThermoFisher), and filled with culture medium (components described below). The agarose layer had a hemispherical depression in the center of the dish made with a sterile 10 mm acrylic necklace bead before gel solidification. The 10mm hemispherical depression is essential to maintain the normal shape of the yolk mass once the embryos are outside their egg case. Embryos were then extracted from their egg cases (*S. officinalis* are housed individually, one embryo per egg case) very slowly and with extreme care to avoid rupturing the yolk mass at the vegetal pole of the egg and were carefully placed in the hemispherical depression in the agarose. To extract the embryo, a single 5mm diameter hole was created in the egg case, which generates a burst of the vitelline liquid and part of the embryo out from the egg case. With the hole kept open, the spontaneous shrinkage of the egg case aided in the expelling of the large cuttlefish embryo. Of every ten eggs prepared this way, between two and five embryos were damaged and had to be discarded. Embryos were cultured at 17^{o}C.

Protein carrier beads and tissue grafting

For protein carrier bead implantation, 150µm diameter Affi-Gel Blue Gel beads (153-7301, Biorad) were selected and transferred to 1mg/ml recombinant human Noggin protein (6057-NG, R&D Systems) in PBS and incubated for 30 minutes to 1 hour at ambient temperature before being implanted in embryos. Control beads were incubated in PBS only.

Grafts of *Hh*-expressing tissue were performed using stage 24 donor embryos and carefully dissecting the funnel side of the mantle-funnel locking system, which carries the *Hh*-expressing thickened funnel epithelium (Tarazona et al., 2016). The dissected tissue was transferred to 10 mg/ml Dispase II (D4693, Sigma) in cuttlefish culture medium and incubated for 40 minutes or until the thickened epithelium was easily detaching from the underlying mesenchyme with the aid of forceps. Tissue was then transferred to cuttlefish culture medium without Dispase II, where they were washed and then grafted into limb buds of stage 17 host embryos. Control grafts were performed using the non-*Hh* expressing epithelium of the funnel.

After bead implantation or tissue grafts, embryos were incubated at 17^{o}C until control embryos reached stage 26, at which point all embryos were collected and prepared for SEM or ISH.

Cuttlefish culture medium

We used a modified version of a cell culture medium for squid neuron, glia and muscle cells that was previously described (Rice et al., 1990). Cuttlefish culture medium had no glucose, was buffered with 20mM HEPES and adjusted the pH to 7.6. The medium contained: 430 mM NaCl, 10 mM KCl, 10 mM CaCl2, 50 mM MgCl2, 1X MEM Non-Essential Amino Acids Solution (11140-076, Life Technologies), 1X MEM Amino Acids Solution (11130-051, Life Technologies), 1X MEM Vitamin Solution (11120-052, Life Technologies), 2 mM L-Glutamine (25030-081, Life Technologies). The medium was

supplemented with 20% heat inactivated fetal bovine serum (16000044, ThermoFisher) and 1X antibiotic/antimycotic solution (A5955, Sigma).

Treatments with small-molecule inhibitors

Cyclopamine treatments were performed as described previously (Tarazona et al., 2016) with the following modifications; stage 16 embryos were treated with 10 μM cyclopamine (C988400, Toronto Research Chemicals) for 2 days, then washed thoroughly ten times with FASW. Embryos were then washed 5 more times every hour and one time every day before collecting the embryos for SEM. Control embryos were treated with 0.1% DMSO and then washed as described above.

Acknowledgments

We thank Emily Merton for technical support, Karen L. Kelley and Kimberly L. Backer-Kelley (UF ICBR) for assistance with electron microscopy, and members of our laboratory for helpful comments and discussions. O.A.T. was supported by a Howard Hughes Medical Institute International Student Research Fellowship, D.H.L. by a Society for Developmental Biology “Choose Development!” fellowship, and L.A.S. by an EDEN Undergraduate Internship.

Funding

This project was supported by an award from the Howard Hughes Medical Institute (to M.J.C).

Competing Interests

The authors declare no competing or financial interests.

Author Contributions

O.A.T. and M.J.C. designed the experiments, analyzed the data and wrote the paper. All authors collaborated in reviewing and editing the paper. O.A.T., D.H.L. and L.A.S. cloned the *Sepia* genes and analyzed gene and protein expression. O.A.T. performed the molecular phylogenetic analyses, scanning electron microscopy, optical projection tomography scanning, three-dimensional reconstructions, *ex-ovo* embryo culture, bead implantation, tissue grafting, and small-molecule treatments.

Supplementary Materials

Figure 1 - figure supplement 1;

Figure 1 - Supplementary Movies 1 to 5

Figure 2 - figure supplements 1 to 10

Figure 2 - Supplementary file 1

Figure 3 - figure supplement 1

Figure 3 - figure supplement 2

Figure 3 - Supplementary file 1

Figure 4 - figure supplement 1

Figure 5 - figure supplement 1

References

Ahn, K., Mishina, Y., Hanks, M.C., Behringer, R.R., Crenshaw, E.B., 3rd, 2001. BMPR-IA signaling is required for the formation of the apical ectodermal ridge and dorsal-ventral patterning of the limb. Development 128, 4449-4461.

Angelini, D.R., Kaufman, T.C., 2005. Insect appendages and comparative ontogenetics. Dev Biol 286, 57-77.

Arnold, J.M., 1965. Normal Embryonic Stages of the Squid, Loligo pealii (Lesueur). Biological Bulletin 128, 24-32.

Arnold, J.M., 1990. Embryonic Development of the Squid, in: Adelman, W.J., Arnold, J.M., Gilbert, D.L. (Eds.), Squid as Experimental Animals. Springer US.

Basler, K., Struhl, G., 1994. Compartment boundaries and the control of Drosophila limb pattern by hedgehog protein. Nature 368, 208-214.

Beermann, A., Jay, D.G., Beeman, R.W., Hulskamp, M., Tautz, D., Jurgens, G., 2001. The Short antennae gene of Tribolium is required for limb development and encodes the orthologue of the Drosophila Distal-less protein. Development 128, 287-297.

Bolognesi, R., Beermann, A., Farzana, L., Wittkopp, N., Lutz, R., Balavoine, G., Brown, S.J., Schroder, R., 2008. Tribolium Wnts: evidence for a larger repertoire in insects with overlapping expression patterns that suggest multiple redundant functions in embryogenesis. Dev Genes Evol 218, 193-202.

Brook, W.J., Cohen, S.M., 1996. Antagonistic interactions between wingless and decapentaplegic responsible for dorsal-ventral pattern in the Drosophila Leg. Science 273, 1373-1377.

Brown, S.J., Patel, N.H., Denell, R.E., 1994. Embryonic expression of the single Tribolium engrailed homolog. Dev Genet 15, 7-18.

Capellini, T.D., Di Giacomo, G., Salsi, V., Brendolan, A., Ferretti, E., Srivastava, D., Zappavigna, V., Selleri, L., 2006. Pbx1/Pbx2 requirement for distal limb patterning is mediated by the hierarchical control of Hox gene spatial distribution and Shh expression. Development 133, 2263-2273.

Choi, K.S., Lee, C., Maatouk, D.M., Harfe, B.D., 2012. Bmp2, Bmp4 and Bmp7 are co-required in the mouse AER for normal digit patterning but not limb outgrowth. PLoS One 7, e37826.

Cohn, M.J., 2011. Development of the external genitalia: conserved and divergent mechanisms of appendage patterning. Dev Dyn 240, 1108-1115.

Cygan, J.A., Johnson, R.L., McMahon, A.P., 1997. Novel regulatory interactions revealed by studies of murine limb pattern in Wnt-7a and En-1 mutants. Development 124, 5021-5032.

Damen, W.G., 2002. Parasegmental organization of the spider embryo implies that the parasegment is an evolutionary conserved entity in arthropod embryogenesis. Development 129, 1239-1250.

589 Diaz-Benjumea, F.J., Cohen, B., Cohen, S.M., 1994. Cell interaction between compartments
590 establishes the proximal-distal axis of Drosophila legs. Nature 372, 175-179.

591 Donoughe, S., Extavour, C.G., 2016. Embryonic development of the cricket Gryllus
592 bimaculatus. Dev Biol 411, 140-156.

593 Gonzalez-Lazaro, M., Rosello-Diez, A., Delgado, I., Carramolino, L., Sanguino, M.A.,
594 Giovinazzo, G., Torres, M., 2014. Two new targeted alleles for the comprehensive analysis of
595 Meis1 functions in the mouse. Genesis 52, 967-975.

596 Gredler, M.L., Larkins, C.E., Leal, F., Lewis, A.K., Herrera, A.M., Perriton, C.L., Sanger, T.J.,
597 Cohn, M.J., 2014. Evolution of external genitalia: insights from reptilian development. Sex Dev
598 8, 311-326.

599 Grimaldi, A., Tettamanti, G., Acquati, F., Bossi, E., Guidali, M.L., Banfi, S., Monti, L.,
600 Valvassori, R., de Eguileor, M., 2008. A hedgehog homolog is involved in muscle formation and
601 organization of Sepia officinalis (mollusca) mantle. Dev Dyn 237, 659-671.

602 Grimmel, J., Dorresteijn, A.W., Frobius, A.C., 2016. Formation of body appendages during
603 caudal regeneration in Platynereis dumerilii: adaptation of conserved molecular toolsets.
604 EvoDevo 7, 10.

605 Hogvall, M., Budd, G.E., Janssen, R., 2018. Gene expression analysis of potential morphogen
606 signalling modifying factors in Panarthropoda. EvoDevo 9, 20.

607 Janssen, R., Prpic, N.M., Damen, W.G., 2004. Gene expression suggests decoupled dorsal
608 and ventral segmentation in the millipede Glomeris marginata (Myriapoda: Diplopoda). Dev Biol
609 268, 89-104.

610 Jiang, J., Struhl, G., 1996. Complementary and Mutually Exclusive Activities of
611 Decapentaplegic and Wingless Organize Axial Patterning during Drosophila Leg Development.
612 Cell 86, 401-409.

613 Kawakami, Y., Esteban, C.R., Matsui, T., Rodriguez-Leon, J., Kato, S., Izpisua Belmonte, J.C.,
614 2004. Sp8 and Sp9, two closely related buttonhead-like transcription factors, regulate Fgf8
615 expression and limb outgrowth in vertebrate embryos. Development 131, 4763-4774.

616 Kojima, T., Michiue, T., Orihara, M., Saigo, K., 1994. Induction of a mirror-image duplication of
617 anterior wing structures by localized hedgehog expression in the anterior compartment of
618 Drosophila melanogaster wing imaginal discs. Gene 148, 211-217.

619 Konigsmann, T., Turetzek, N., Pechmann, M., Prpic, N.M., 2017. Expression and function of
620 the zinc finger transcription factor Sp6-9 in the spider Parasteatoda tepidariorum. Dev Genes
621 Evol 227, 389-400.

622 Kroger, B., Vinther, J., Fuchs, D., 2011. Cephalopod origin and evolution: A congruent picture
623 emerging from fossils, development and molecules. BioEssays : news and reviews in
624 molecular, cellular and developmental biology 33, 602-613.

625 Lecuit, T., Cohen, S.M., 1997. Proximal-distal axis formation in the Drosophila leg. Nature 388,
626 139-145.

627 Lee, P.N., Callaerts, P., de Couet, H.G., Martindale, M.Q., 2003. Cephalopod Hox genes and
628 the origin of morphological novelties. Nature 424, 1061-1065.

629 Lemaire, J., 1970. Table de developpement embryonnaire de Sepia officinalis. L. (Mollusque
630 Cephalopode). Bull Soc Zool France, 95:773–782. .

631 Lemons, D., Fritzenwanker, J.H., Gerhart, J., Lowe, C.J., McGinnis, W., 2010. Co-option of an
632 anteroposterior head axis patterning system for proximodistal patterning of appendages in
633 early bilaterian evolution. Dev Biol 344, 358-362.

634 Lewis, P.M., Dunn, M.P., McMahon, J.A., Logan, M., Martin, J.F., St-Jacques, B., McMahon,
635 A.P., 2001. Cholesterol modification of sonic hedgehog is required for long-range signaling
636 activity and effective modulation of signaling by Ptc1. Cell 105, 599-612.

637 Loomis, C.A., Kimmel, R.A., Tong, C.X., Michaud, J., Joyner, A.L., 1998. Analysis of the
638 genetic pathway leading to formation of ectopic apical ectodermal ridges in mouse Engrailed-1
639 mutant limbs. Development 125, 1137-1148.

640 Mercader, N., Leonardo, E., Azpiazu, N., Serrano, A., Morata, G., Martinez-A, C., Torres, M.,
641 1999. Conserved regulation of proximodistal limb axis development by Meis1/Hth. Nature 402,
642 425-429.

643 Minelli, A., 2000. Limbs and tail as evolutionarily diverging duplicates of the main body axis.
644 Evolution & development 2, 157-165.

645 Minelli, A., 2003. The Development of Animal Form: Ontogeny, Morphology, and Evolution.
646 Cambridge University Press.

647 Moczek, A.P., Nagy, L.M., 2005. Diverse developmental mechanisms contribute to different
648 levels of diversity in horned beetles. Evolution & development 7, 175-185.

649 Moczek, A.P., Rose, D., Sewell, W., Kesselring, B.R., 2006. Conservation, innovation, and the
650 evolution of horned beetle diversity. Dev Genes Evol 216, 655-665.

651 Nielsen, C., 2012. Animal Evolution: Interrelationships of the Living Phyla. OUP Oxford.

652 Nödl, M.T., Kerbl, A., Walzl, M.G., Müller, G.B., de Couet, H.G., 2016. The cephalopod arm
653 crown: appendage formation and differentiation in the Hawaiian bobtail squid Euprymna
654 scolopes. Front Zool 13, 44.

655 Panganiban, G., Irvine, S.M., Lowe, C., Roehl, H., Corley, L.S., Sherbon, B., Grenier, J.K.,
656 Fallon, J.F., Kimble, J., Walker, M., Wray, G.A., Swalla, B.J., Martindale, M.Q., Carroll, S.B.,
657 1997. The origin and evolution of animal appendages. Proc Natl Acad Sci U S A 94, 5162-
658 5166.

659 Parr, B.A., McMahon, A.P., 1995. Dorsalizing signal Wnt-7a required for normal polarity of D-V
660 and A-P axes of mouse limb. Nature 374, 350-353.

661 Prpic, N.M., 2004. Homologs of wingless and decapentaplegic display a complex and dynamic
662 expression profile during appendage development in the millipede Glomeris marginata
663 (Myriapoda: Diplopoda). Front Zool 1, 6.

664 Prpic, N.M., 2008. Parasegmental appendage allocation in annelids and arthropods and the
665 homology of parapodia and arthropodia. Front Zool 5, 17.

666 Prpic, N.M., Janssen, R., Wigand, B., Klingler, M., Damen, W.G., 2003. Gene expression in
667 spider appendages reveals reversal of exd/hth spatial specificity, altered leg gap gene
668 dynamics, and suggests divergent distal morphogen signaling. Dev Biol 264, 119-140.

669 Prpic, N.M., Tautz, D., 2003. The expression of the proximodistal axis patterning genes Distal-
670 less and dachshund in the appendages of Glomeris marginata (Myriapoda: Diplopoda)
671 suggests a special role of these genes in patterning the head appendages. Dev Biol 260, 97-
672 112.

673 Prpic, N.M., Wigand, B., Damen, W.G., Klingler, M., 2001. Expression of dachshund in wild-
674 type and Distal-less mutant Tribolium corroborates serial homologies in insect appendages.
675 Dev Genes Evol 211, 467-477.

676 Pueyo, J.I., Couso, J.P., 2005. Parallels between the proximal-distal development of vertebrate
677 and arthropod appendages: homology without an ancestor? Curr Opin Genet Dev 15, 439-446.

678 Rice, R.V., Mueller, R., Adelman, W.J., 1990. Tissue culture of squid neurons, glia, and muscle
679 cells, in: Adelman, W.J., Arnold, J.M., Gilbert, D.L. (Eds.), Squids as experimental animals.
680 Springer US.

681 Riddle, R.D., Johnson, R.L., Laufer, E., Tabin, C., 1993. Sonic hedgehog mediates the
682 polarizing activity of the ZPA. Cell 75, 1401-1416.

683 Ruppert, E.E., Fox, R.S., Barnes, R.D., 2004. Invertebrate Zoology: A Functional Evolutionary
684 Approach. Thomson-Brooks/Cole.

685 Salsi, V., Vigano, M.A., Cocchiarella, F., Mantovani, R., Zappavigna, V., 2008. Hoxd13 binds in
686 vivo and regulates the expression of genes acting in key pathways for early limb and skeletal
687 patterning. Dev Biol 317, 497-507.

688 Sanchez-Salazar, J., Pletcher, M.T., Bennett, R.L., Brown, S.J., Dandamudi, T.J., Denell, R.E.,
689 Doctor, J.S., 1996. The Tribolium decapentaplegic gene is similar in sequence, structure, and
690 expression to the Drosophila dpp gene. Dev Genes Evol 206, 237-246.

691 Schaeper, N.D., Prpic, N.M., Wimmer, E.A., 2010. A clustered set of three Sp-family genes is
692 ancestral in the Metazoa: evidence from sequence analysis, protein domain structure,
693 developmental expression patterns and chromosomal location. BMC Evol Biol 10, 88.

694 Scherz, P.J., McGlinn, E., Nissim, S., Tabin, C.J., 2007. Extended exposure to Sonic hedgehog
695 is required for patterning the posterior digits of the vertebrate limb. Dev Biol 308, 343-354.

696 Setton, E.V.W., Sharma, P.P., 2018. Cooption of an appendage-patterning gene cassette in
697 the head segmentation of arachnids. Proc Natl Acad Sci U S A 115, E3491-E3500.

698 Shapiro, M.D., Hanken, J., Rosenthal, N., 2003. Developmental basis of evolutionary digit loss
699 in the Australian lizard Hemiergis. Journal of experimental zoology. Part B, Molecular and
700 developmental evolution 297, 48-56.

701 Shigeno, S., Sasaki, T., Moritaki, T., Kasugai, T., Vecchione, M., Agata, K., 2008. Evolution of
702 the cephalopod head complex by assembly of multiple molluscan body parts: Evidence from
703 Nautilus embryonic development. Journal of morphology 269, 1-17.

704 Shubin, N., Tabin, C., Carroll, S., 1997. Fossils, genes and the evolution of animal limbs.
705 Nature 388, 639-648.

706 Shubin, N., Tabin, C., Carroll, S., 2009. Deep homology and the origins of evolutionary novelty.
707 Nature 457, 818-823.

708 Smith, S.A., Wilson, N.G., Goetz, F.E., Feehery, C., Andrade, S.C., Rouse, G.W., Giribet, G.,
709 Dunn, C.W., 2011. Resolving the evolutionary relationships of molluscs with phylogenomic
710 tools. Nature 480, 364-367.

711 Tabin, C.J., Carroll, S.B., Panganiban, G., 1999. Out on a Limb: Parallels in Vertebrate and
712 Invertebrate Limb Patterning and the Origin of Appendages. American Zoologist 39, 650-663.

713 Tarazona, O.A., Slota, L.A., Lopez, D.H., Zhang, G., Cohn, M.J., 2016. The genetic program
714 for cartilage development has deep homology within Bilateria. Nature 533, 86-89.

715 Vieux-Rochas, M., Bouhali, K., Mantero, S., Garaffo, G., Provero, P., Astigiano, S., Barbieri, O.,
716 Caratozzolo, M.F., Tullo, A., Guerrini, L., Lallemand, Y., Robert, B., Levi, G., Merlo, G.R., 2013.
717 BMP-mediated functional cooperation between Dlx5;Dlx6 and Msx1;Msx2 during mammalian
718 limb development. PLoS One 8, e51700.

719 Winchell, C.J., Jacobs, D.K., 2013. Expression of the Lhx genes apterous and lim1 in an errant
720 polychaete: implications for bilaterian appendage evolution, neural development, and muscle
721 diversification. EvoDevo 4, 4.

722 Winchell, C.J., Valencia, J.E., Jacobs, D.K., 2010. Expression of Distal-less, dachshund, and
723 optomotor blind in Neanthes arenaceodentata (Annelida, Nereididae) does not support
724 homology of appendage-forming mechanisms across the Bilateria. Dev Genes Evol 220, 275-
725 295.

726 Witte, F., Dokas, J., Neuendorf, F., Mundlos, S., Stricker, S., 2009. Comprehensive expression
727 analysis of all Wnt genes and their major secreted antagonists during mouse limb development
728 and cartilage differentiation. Gene Expr Patterns 9, 215-223.

729 Zhu, J., Nakamura, E., Nguyen, M.T., Bao, X., Akiyama, H., Mackem, S., 2008. Uncoupling
730 Sonic hedgehog control of pattern and expansion of the developing limb bud. Developmental
731 cell 14, 624-632.
732

Figure Legends

Figure 1. Development of arms and tentacles in the cuttlefish, *Sepia officinalis*. (**A**) Phylogenetic relationships of Mollusca based on phylogenomic data (Smith et al., 2011) illustrating the unique morphology of the cephalopod body plan compared to other mollusks. (**B**) OPT reconstruction of a cuttlefish hatchling showing positions of the limbs; only arms are visible (see also Supplementary Movie 1). (**C** to **D**), SEM of the ventral side of a cuttlefish arm (C) and tentacle (D). Suckers are pseudocolored blue. Note distal restriction of suckers in tentacle relative to arm. (**E**) OPT reconstruction illustrating the internally retracted tentacles. Specimens are same as in (B), but here the tentacles are displayed in orange and the rest of the tissue is rendered translucent (see also Supplementary Movie 2). (**F** and **G**) Phospho-histone H3 (PHH3) immunostaining at stage 15 shows localized clusters of proliferating cells at the onset of limb development (black arrowheads) but little proliferation in the interlimb region (open arrowhead). (F) PHH3 detection by colorimetric reaction with DAB in a whole mount. (G) PHH3 immunofluorescence (red) on limb cryosection (white bracket). Cell nuclei (blue) are labeled by Hoechst staining. (**H** and **L**) OPT reconstructions of cuttlefish embryos at stages 16 to 24. Cuttlefishes have five bilaterally symmetric limb pairs (ten limbs; eighth arms and two tentacles). Numbered arrowheads mark all five limbs/limb buds on the left side of each embryo. The left tentacle differentiates from position number four (orange arrowhead), whereas arms form from limb buds at the other positions (yellow arrowheads). See also Supplementary Movies 3-5. A, anterior; P, posterior; D, dorsal; V, ventral; Stm, stomodeum; Mnt, mantle. (**M** to **O**) SEM during early stages of cuttlefish limb development (stages 16 to 19). Morphogenesis of the limb is first observed as a slight swelling (M) that transforms into a limb bud (O) as proximodistal outgrowth progresses. D, dorsal; V, ventral. **p-s**, SEM at later stages of cuttlefish limb development (stages 21 to 25) showing the formation of sucker buds on the ventral surface of a developing limb. A primordial sucker band (yellow arrows) is observed along the ventral midline of a stage 21 limb bud (P). At later stages, the band cleaves superficially from the proximal end to form the sucker buds (pseudocolored blue in Q to S). Scale bars: 0.5 mm (C and D) and 100 µm (M to S).

Figure 2. Molecular regionalization of proximodistal, anteroposterior, and dorsovental axes during cephalopod limb development. (**A**) OPT reconstruction of cuttlefish embryo at stage 20 showing all five limb buds on the left side of the embryo (arms, yellow arrowheads; tentacle, orange arrowhead). (**B** to **E**) OPT reconstructions showing four representative genes with polarized expression patterns along major axes of limb buds (gene expression indicated by orange/yellow). Proximodistally polarized expression of *Exd* (B) and *Wnt5* (C). Anteroposteriorly polarized expression of *Hh* (D**),** dorsoventrally polarized expression of *Bmp2/4* (E). (**F** to **O**), *In situ* hybridizations of cuttlefish limb buds at stage 17 (left) and stage 20 (right) showing polarized patterns of expression along the proximodistal axis for *Exd* (F), *Hth* (G), *Dll* (H), *Dac* (I) and *Sp8/9* (J); the anteroposterior axis for *Hh* (K) and *Ptc* (L); and the dorsoventral axis for *Bmp2/4* (M), *En* (N) and *Sfrp1/2/5* (O). A, anterior; P, posterior; D, dorsal; V, ventral; Di, distal; Pr, proximal.

Figure 3. Expression of proximal identity genes *Exd* and *Hth* in arms and tentacles corresponds with distribution of suckers; Wnt signaling repressors are dorsally restricted. (A and **B**) Compared to arms (A), tentacles (B) show a distally expanded domain of *Exd* expression in the proximal region of the limb. (**C** and **D**) A similar pattern of expression is detected for *Hth* during arm (C) and tentacle (D) development. Distal boundary of *Exd* and *Hth* expression marked by black arrowheads in (A to D). (**E**) Expanded expression of proximal identity genes correlates with the expanded sucker-free domain seen in tentacles compared to arms. (**F** and **H**) The Wnt ligands *Wnt1*, *Wnt5* and *Wnt7* show a distally restricted expression but no dorsoventral polarization at stages 17 and 20. (**I**) The Wnt signaling transcription factor *Tcf3/4* is also distally restricted but shows no dorsoventral polarization at stages 17 and 20. (**J** and **K)** Fluorescent nuclear stain SYBR Safe highlights limb buds (yellow arrowheads). Boxed region in (J) is enlarged in (K); white arrowhead marks interlimb region. (**L** and **M**) The Wnt ligand repressors *Notum* and *Sfrp1/2/5* are expressed in the dorsal interlimb region (black arrowhead in L and M; compare with K). *Sfrp1/2/5* expression expands into the dorsal limb bud (black arrows in M) in stage 19 embryos, whereas *Notum* stays dorsal

but proximally restricted (open arrowheads mark the limb buds in L). (**N** and **O**) The earliest sign of sucker formation can be detected by SEM as a slight swelling (N) and by *Notum* expression (O) on the ventral side of stage 21 limb buds. (**P** and **Q)** Expression of *Notum* is maintained through later stages of sucker morphogenesis, as seen in stage 26 tentacles (lateral views).

Figure 4. Bmp signaling controls dorsoventral patterning and Hh signaling regulates anteroposterior patterning of cuttlefish limbs. (**A** to **C**) Implantation of carrier beads loaded with the Bmp inhibitor Noggin (A) results in formation of ectopic sucker buds (n=8/12) on the dorsal surface of the limb (B), whereas PBS control beads (n=15/15) result in normal development of the dorsal limb (pseudocolored red) restriction of suckers (pseudocolored blue) to the ventral side of the limb (C). (**D** to **F**), *Hh*-expressing cells (taken from the funnel of a stage 24 donor embryo) grafted to the posterior side of a stage 17 cuttlefish limb bud (D) generates a posterior mirror-image limb duplication (n=7/12; yellow arrow in E), whereas no duplication (n=8/8) results when control (Hh-negative) cells are grafted to the same position (F). Sucker buds are pseudocolored blue in (E and F); sucker buds in duplicated limb marked with a white arrowhead. (**G** and **H**) Noggin beads induce ectopic expression of *Notum* on the dorsal side of the limb (G). Limbs receiving control PBS beads show normal expression of *Notum* ventrally (H). (**I** and **J**) Graft of *Hh*-expressing tissue to the posterior side of the limb induces ectopic domain of *Notum* prior to duplication of the limb (I; black arrowhead). Note the two separate domains of *Notum* expression in I compared to a single *Notum* expression domain in the limb with the *Hh*-negative control graft (J). (**K** to **P**) Transitory repression of Hh signaling by cyclopamine (K) during early stages of limb development disrupts the anteroposterior distribution of sucker bud rows (L, N, O). Cyclopamine-treated limbs showing complete loss of suckers in tentacles (L) and reduction in the number of sucker bud rows in arms (N and O). Control embryos treated with vehicle only (DMSO) develop the normal number of sucker bud rows in tentacles (M) and arms (P). Sucker buds are pseudocolored blue in (B, E, F, and M- P). Scale bars 100 μm.

Figure 5. Molecular patterning of the anteroposterior, proximodistal, and dorsoventral axes of developing limbs in vertebrates, arthropods, and cephalopods. For each lineage, the top row shows schematic representations of a generalized limb bud and an adult limb in two different orientations. Axes are indicated to the left of each limb bud (A, anterior; Po, posterior; Pr, proximal; Di, distal; Do, dorsal; Ve, ventral) Bottom rows show limb buds with gene expression domains pink color). Vertebrate gene expression based on mouse limb development. Arthropod gene expression is a compound reconstruction from chelicerate, myriapod, and hexapod limb development in order to consolidate a complete set of pro-orthologous genes comparable to vertebrate and cephalopod lineages. Cephalopod gene expression is based on findings in this study from the cuttlefish *Sepia officinalis* and *Sepia bandensis*. The figure illustrates the conserved and divergent expression patterns of homologous (pro-orthologous) genes, some of which share equivalent roles in patterning the limb axes. The proximodistal axis displays conserved expression of transcription factors at opposite ends; *Htx* (pro-ortholog of vertebrate *Meis* genes) and *Exd* (pro-ortholog of vertebrate *Pbx* genes) are restricted proximally, whereas *Dll* (pro-ortholog of vertebrate *Dlx* genes), *Wnt5* (pro-ortholog of *Wnt5a*) and *Sp8/9* (pro-ortholog of vertebrate *Sp8* and *Sp9* genes, known as *Sp6-9* in some arthropods) show distally restricted expression. The typical expression pattern of *Dac* seen in arthropods (between proximally and distally restricted genes) is not strictly conserved in vertebrates (*Dac* pro-ortholog of vertebrate *Dach* genes) or cephalopods. However, *Dac* expression in non-locomotory arthropod appendages (e.g., mandibles) is distally restricted, resembling cephalopod *Dac* expression (Donoughe and Extavour, 2016). Expression patterns of the diverse family of *Wnt* genes shows interesting variation. Although, some members of the family show variation in their expression pattern (*Wnt1* and *Wnt7*), there is a general pattern of distal restriction of Wnt expression (represented here by *Wnt5*, but also seen in many other Wnt ligands)in the three lineages. At the level of individual Wnt members, *Wg* (pro-ortholog of vertebrate *Wnt1*) is restricted ventrally in arthropods but not in vertebrates or cephalopods, and *Wnt7a* (arthropod and cephalopod *Wnt7* genes are pro-orthologs of vertebrate *Wnt7a*) is restricted dorsally in vertebrates but not in arthropods or cephalopods. Restricted expression of Wnt ligands either dorsally or

ventrally has not been reported in cephalopods, but the dorsally restricted expression of the Wnt repressor *Sfrp1/2/5* suggests a role of polarized Wnt pathway activation in the control of the dorsoventral axis of cephalopod limbs, similar to vertebrates (by dorsal *Wnt7a*) and arthropods (by ventral *Wg*). There is a clear restriction of at least one Bmp ligand (vertebrate *Bmp7* and cephalopod *Bmp2/4*; pro-orthologs of arthropod *Dpp*) and the transcription factor *En* along the dorsoventral axis in these three lineages. Finally, polarized expression of *Hh* is conserved in the three lineages (posterior in vertebrates and arthropods, but anterior in cephalopods), which, together with the functional manipulations, indicates conservation of Hh signaling in patterning the anteroposterior limb axis in the three lineages. The asterisk (*) in arthropod *Dac* indicates that some mouth appendages show a distal expression domain (Donoughe and Extavour, 2016) (Angelini and Kaufman, 2005) more similar to cephalopod *Dac* limb expression than to *Dac* expression in arthropod legs. Two asterisks (**) indicate that *Wnt5* expression show variation in arthropods, with a sub-distal expression in chelicerates (Damen, 2002) but distal in hexapods (i.e. flour beetle) (Bolognesi et al., 2008). Three asterisks (***) indicate that *Dpp* shows variation in its expression domain in arthropods, in some hexapods and chelicerates showing a distal expression domain whereas in Myriapods and other hexapods it is dorsally restricted as depicted here (Angelini and Kaufman, 2005). Schematized gene expression domains for vertebrates and arthropods are from the following sources. Mouse gene expression: *Meis1* (Gonzalez-Lazaro et al., 2014), *Pbx1* (Capellini et al., 2006), *Sp8* (Kawakami et al., 2004), *Dlx5* (Vieux-Rochas et al., 2013), *Dach1* (Salsi et al., 2008), *Wnt1*, *Wnt5a*, *Wnt7a*, *Sfrp2* (Witte et al., 2009), *Shh* (Riddle et al., 1993), *Bmp7* (Choi et al., 2012) and *En1* (Loomis et al., 1998). Arthropod expression based on: Chelicerates, *Htx*, *Exd*, *Dll*, *Dac* (Prpic et al., 2003), *Sp8/9* (Konigsmann et al., 2017), *Wg* (Damen, 2002), *En* (Damen, 2002) and *Sfrp1*/2/5 (Hogvall et al., 2018); Myriapods, *Htx*, *Exd*, *Dll*, *Dac* (Prpic and Tautz, 2003), *Sp8*/*9* (Setton and Sharma, 2018), *Wg*, *Dpp* (Prpic, 2004), *Wnt5*, *Wnt7*, *Hh*, *En* (Janssen et al., 2004), *Sfrp1/2/5* (Hogvall et al., 2018); Hexapods, flour beetle, *Htx* , *Exd* (Prpic et al., 2003), *Sp8*/*9* (Schaeper et al., 2010), *Dll* (Beermann et al., 2001), *Dac* (Prpic et al., 2001), *Wg*, *Wnt5* (Bolognesi et al., 2008), *Dpp* (Sanchez-Salazar et al., 1996), *En*

887 (Brown et al., 1994); Hexapods, cricket, *Htx*, *Exd*, *Dll*, *Dac*, *Wg*, *Hh*, *Dpp*, *En* (Donoughe
888 and Extavour, 2016).

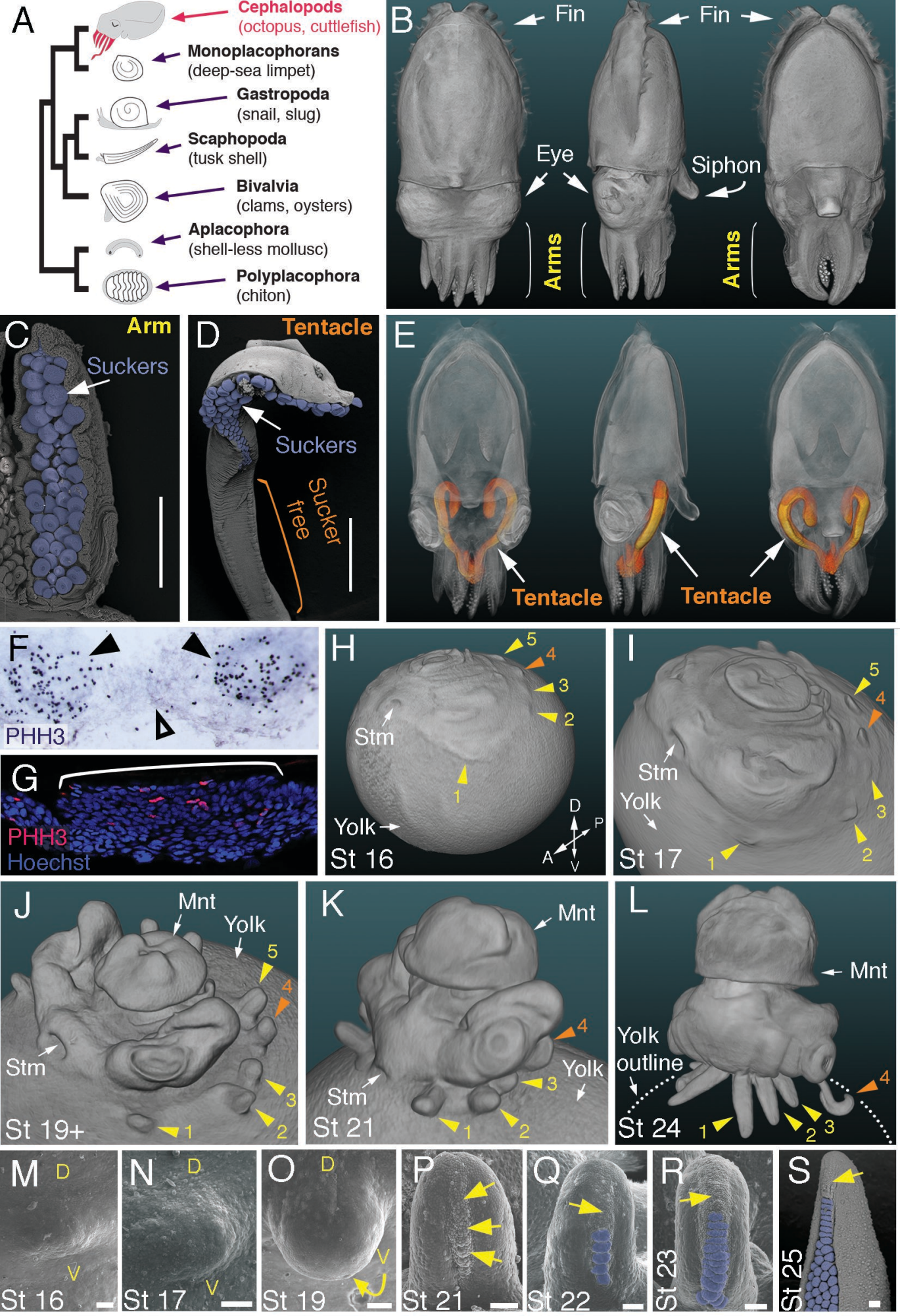
A
Cephalopods
(octopus, cuttlefish)
Monoplacophorans
(deep-sea limpet)
Gastropoda
(snail, slug)
Scaphopoda
(tusk shell)
Bivalvia
(clams, oysters)
Aplacophora
(shell-less mollusc)
Polyplacophora
(chiton)
B
Fin
Fin
Eye
Siphon
Arms
Arms
C
Arm
Suckers
D
Tentacle
Suckers
Sucker free
E
Tentacle
Tentacle
F
PHH3
G
PHH3
Hoechst
H
Stm
Yolk
St 16
I
Stm
Yolk
St 17
J
Mnt
Yolk
Stm
St 19+
K
Mnt
Stm
Yolk
St 21
L
Mnt
Yolk
outline
St 24
M
St 16
N
St 17
O
St 19
P
St 21
Q
St 22
R
St 23
S
St 25

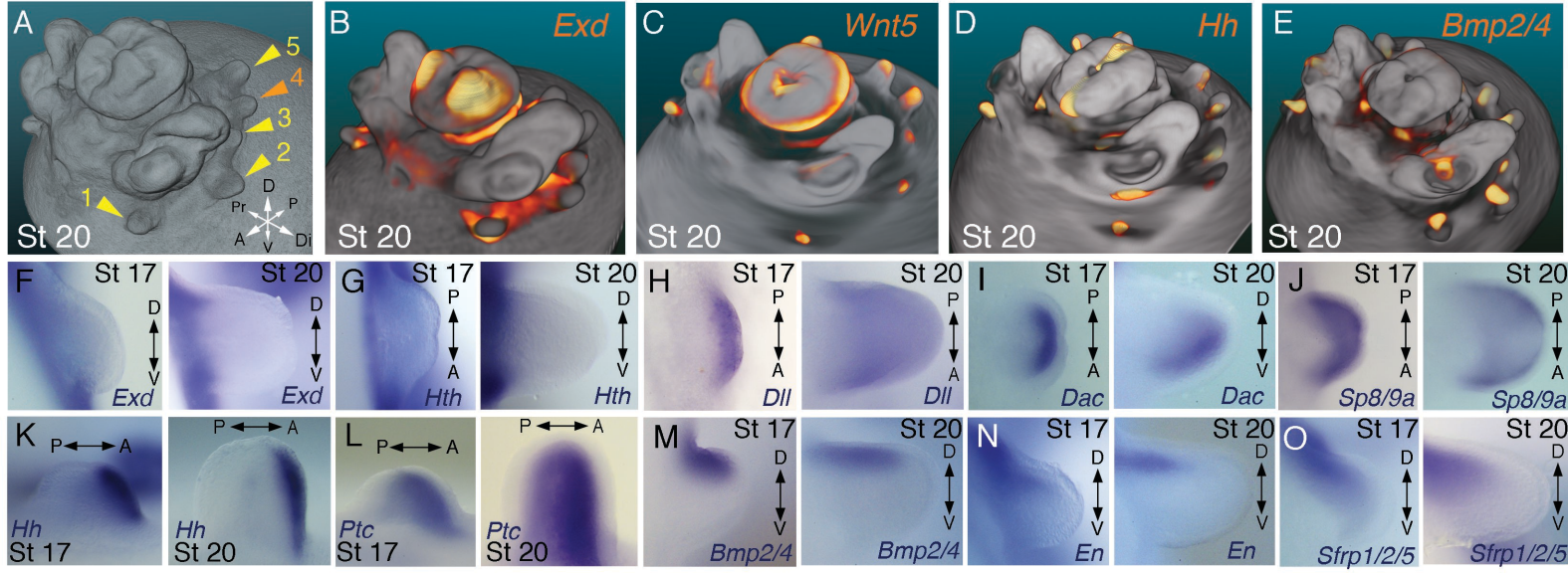
A
5
4
3
2
1
D
Pr
P
A
V
Di
St 20
B
Exd
St 20
C
Wnt5
St 20
D
Hh
St 20
E
Bmp2/4
St 20
F
St 17
D
V
Exd
St 20
D
V
Exd
G
St 17
P
A
Hth
St 20
D
V
Hth
H
St 17
P
A
Dll
St 20
P
A
Dll
I
St 17
P
A
Dac
St 20
D
V
Dac
J
St 17
P
A
Sp8/9a
St 20
P
A
Sp8/9a
K
P
A
Hh
St 17
P
A
Hh
St 20
L
P
A
Ptc
St 17
P
A
Ptc
St 20
M
St 17
D
V
Bmp2/4
St 20
D
V
Bmp2/4
N
St 17
D
V
En
St 20
D
V
En
O
St 17
D
V
Sfrp1/2/5
St 20
D
V
Sfrp1/2/5

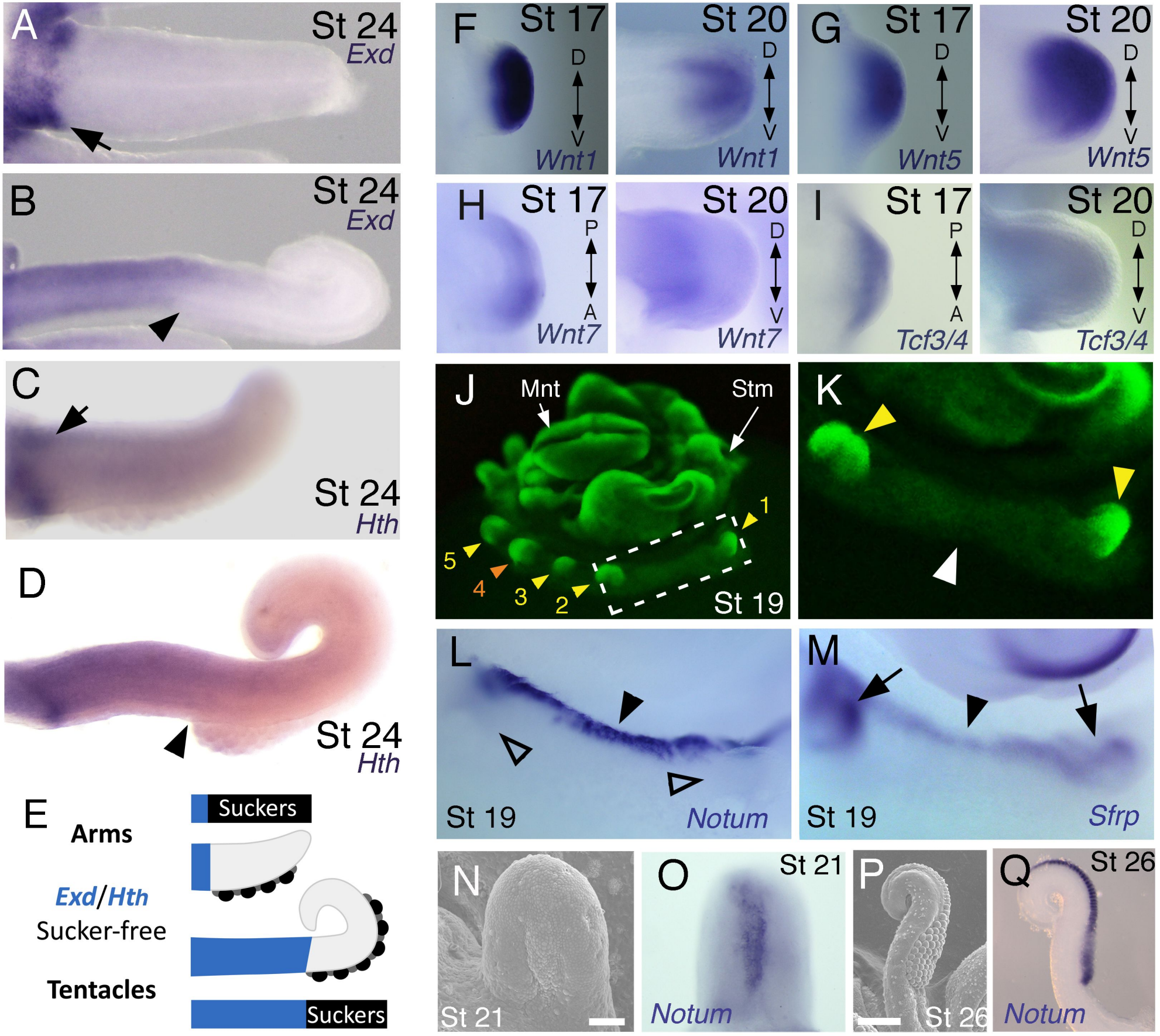
A
St 24
Exd
B
St 24
Exd
C
St 24
Hth
D
St 24
Hth
E
Arms
Exd/Hth
Sucker-free
Tentacles
Suckers
Suckers
F
St 17
D
V
Wnt1
St 20
D
V
Wnt1
G
St 17
D
V
Wnt5
St 20
D
V
Wnt5
H
St 17
P
A
Wnt7
St 20
D
V
Wnt7
I
St 17
P
A
Tcf3/4
St 20
D
V
Tcf3/4
J
Mnt
Stm
1
2
3
4
5
St 19
K
L
St 19
Notum
M
St 19
Sfrp
N
St 21
O
St 21
Notum
P
St 26
Q
St 26
Notum

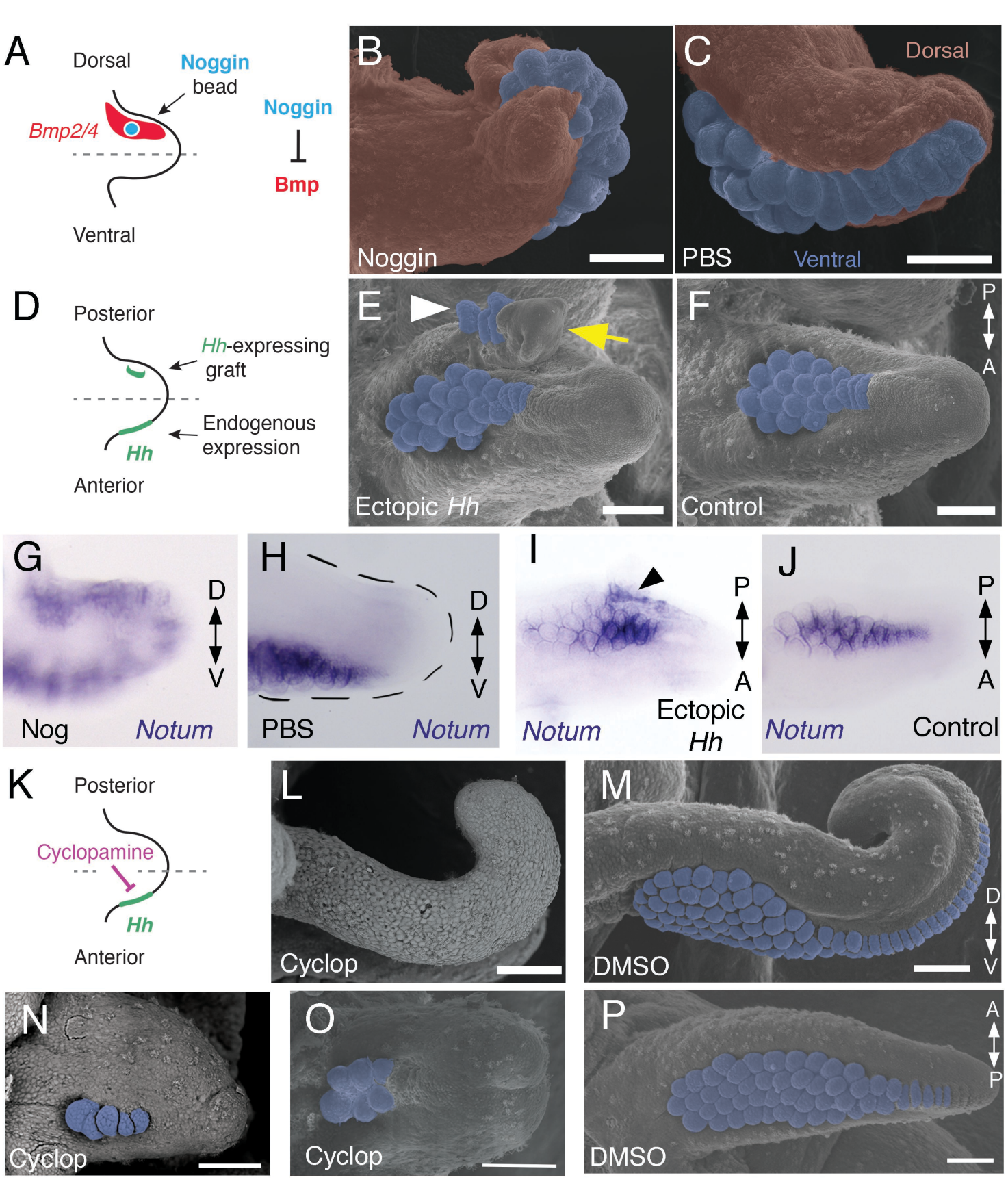
A
Dorsal
Noggin
bead
Bmp2/4
Noggin
Bmp
Ventral
B
Noggin
C
Dorsal
PBS
Ventral
D
Posterior
Hh-expressing
graft
Endogenous
expression
Hh
Anterior
E
Ectopic Hh
F
P
A
Control
G
D
V
Nog
Notum
H
D
V
PBS
Notum
I
P
A
Notum
Ectopic
Hh
J
P
A
Notum
Control
K
Posterior
Cyclopamine
Hh
Anterior
L
Cyclop
M
DMSO
D
V
N
Cyclop
O
Cyclop
P
A
P
DMSO

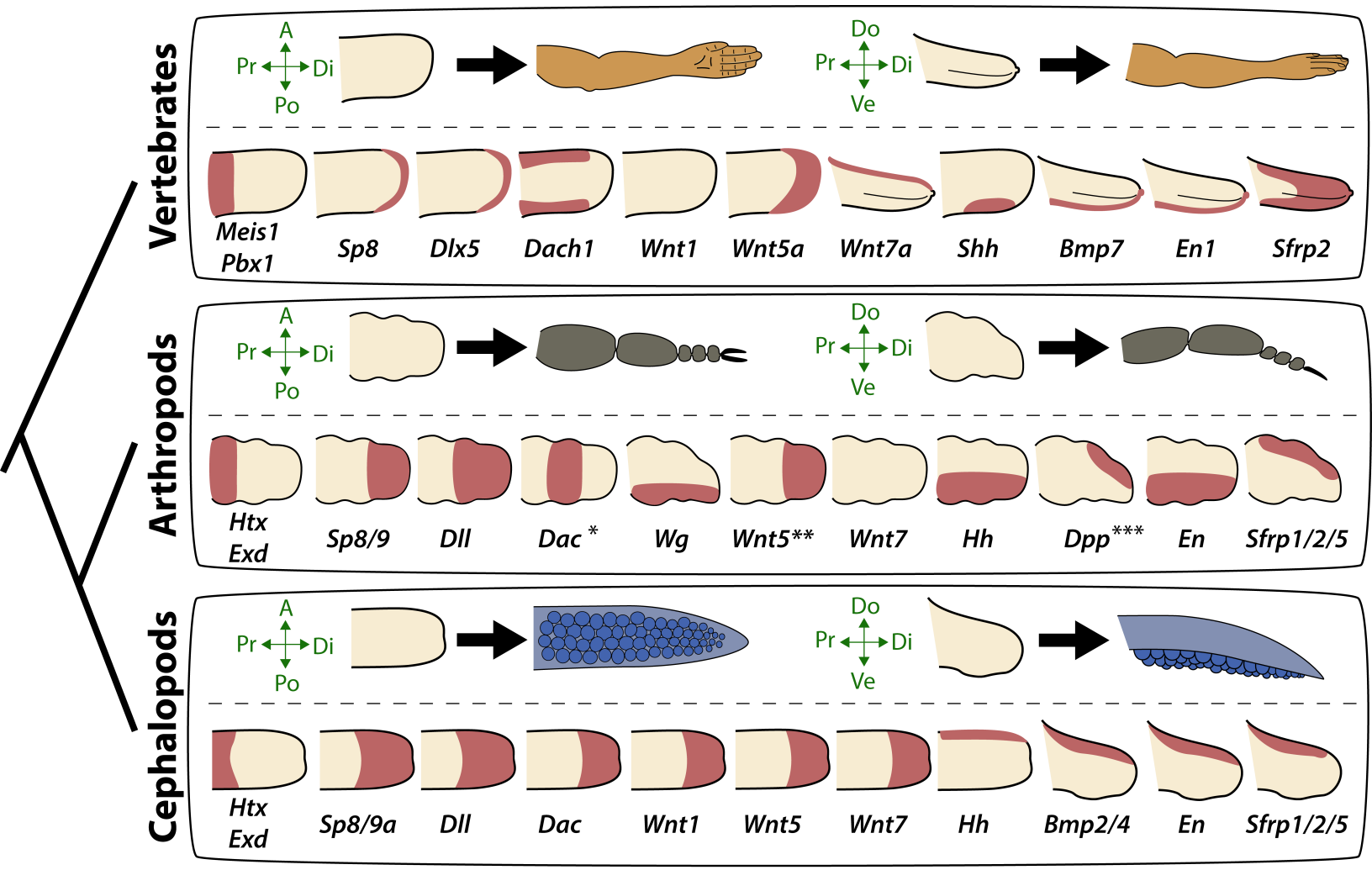

Evolution of limb development in cephalopod mollusks

Authors: Tarazona, Lopez, Slota, and Cohn

Supplementary materials

Figure 1 - figure supplement 1;

Figure 1 - Supplementary Movies 1 to 5

Figure 2 - figure supplements 1 to 10

Figure 2 - Supplementary file 1

Figure 3 - figure supplement 1

Figure 3 – figure supplement 2

Figure 3 – Supplementary file 1

Figure 4 - figure supplement 1

Figure 5 – figure supplement 1

Legends to Figure Supplements

Figure 1 supplements

Figure 1 – figure supplement 1. Sucker morphogenesis. All panels show scanning electron micrographs; scale bars, 100 µm. (**A** and **B**) Sucker buds are arranged in parallel rows along the anteroposterior axis, with four rows in arms (A) and eight rows in tentacles (B). (**C** to **G**) Sucker formation progresses from distal to proximal. Colored squares in c are shown at higher magnification in d-g. Superficial cleavage of the proximal side of the primordial sucker band in (D) and segregation of the recently formed sucker buds in (E). Early sucker bud cells (G) form a dome-shaped outline compared to the rather flattened morphology of the non-sucker forming surface epithelium (F). (**H** and **I**) Higher magnification of sucker buds in a cuttlefish hatchling showing that sucker differentiation is not yet complete in hatchlings (H) compared to the differentiated suckers found in more mature individuals (I), which indicates that a substantial portion of sucker development occurs during post hatchling development.

Figure 1- supplementary movie 1. OPT 3D reconstruction showing cuttlefish hatchling morphology.

Figure 1- supplementary movie 2. OPT 3D reconstruction showing the internal location of the tentacles in a cuttlefish hatchling. Tentacles in orange, other parts of the body in gray (partially translucent).

Figure 1- supplementary movie 3. OPT 3D reconstruction showing morphology of a cuttlefish embryo at stage 17. Embryo is positioned on top of the yolk. The early limb buds (8 arm buds and 2 tentacle buds) can be seen around the margin of the embryo.

Figure 1- supplementary movie 4. OPT 3D reconstruction showing morphology of a cuttlefish embryo at late stage 19.

Figure 1- supplementary movie 5. OPT 3D reconstruction showing the morphology of a cuttlefish embryo at stage 24.

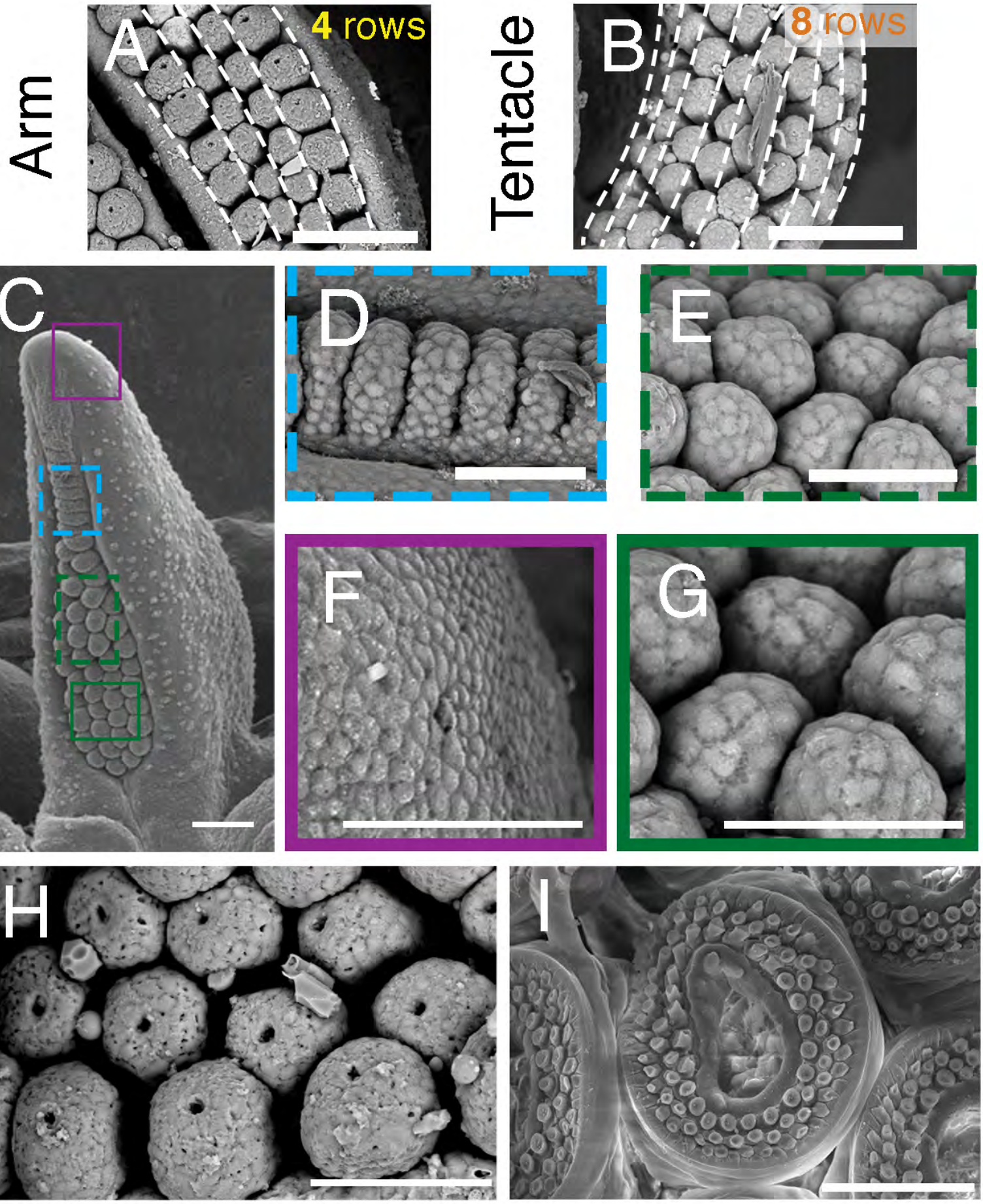

Figure 2 supplements

Figure 2 – figure supplement 1. Molecular phylogenetic reconstruction using maximum likelihood implemented in RAxML of *Wnt* family ligands isolated in this study. Arrows mark the phylogenetic placement of 4 cuttlefish *Wnt* sequences.

Figure 2 – figure supplement 2. Molecular phylogenetic reconstruction using maximum likelihood implemented in RAxML of *Pan*/*Tcf* transcription factors isolated in this study. The arrow marks the phylogenetic placement of one cuttlefish *Tcf* sequences.

Figure 2 – figure supplement 3. Molecular phylogenetic reconstruction using maximum likelihood implemented in RAxML of *Dac/Dach* transcription factors isolated in this study. The arrow marks the phylogenetic placement of one cuttlefish *Dac* sequences.

Figure 2– figure supplement 4. Molecular phylogenetic reconstruction using maximum likelihood implemented in RAxML of *Sp* family of transcription factors isolated in this study. The arrow marks the phylogenetic placement of one cuttlefish *Sp* sequence.

Figure 2 – figure supplement 5. Molecular phylogenetic reconstruction using maximum likelihood implemented in RAxML of Homeodomain family of transcription factors isolated in this study. Arrows mark the phylogenetic placement of 4 cuttlefish Homeodomain sequences.

Figure 2 – figure supplement 6**.** Molecular phylogenetic reconstruction using maximum likelihood implemented in RAxML of *Notum* Wnt inhibitors isolated in this study. The arrow marks the phylogenetic placement of one cuttlefish *Notum* sequence.

Figure 2 – figure supplement 7. Molecular phylogenetic reconstruction using maximum likelihood implemented in RAxML of *Frizzled* Wnt co-receptors and *Sfrp* extracellular Wnt repressors isolated in this study. Arrows mark the phylogenetic placement of one cuttlefish *Frizzled* and one *Sfrp***.**

Figure 2 – figure supplement 8. Molecular phylogenetic reconstruction using maximum likelihood implemented in RAxML of *Tgfβ* family ligands isolated in this study. The arrow marks the phylogenetic placement of cuttlefish *Bmp2/4***.**

Figure 2 – figure supplement 9. Molecular phylogenetic reconstruction using maximum likelihood implemented in RAxML of *Hh* ligand previously isolated (PMID:27111511) in this study. The arrow marks the phylogenetic placement of cuttlefish *Hh* sequence**.**

Figure 2 – figure supplement 10**.** Molecular phylogenetic reconstruction using maximum likelihood implemented in RAxML of Hedgehog *Patch* receptors isolated in this study. The arrow marks the phylogenetic placement of cuttlefish *Patched*.

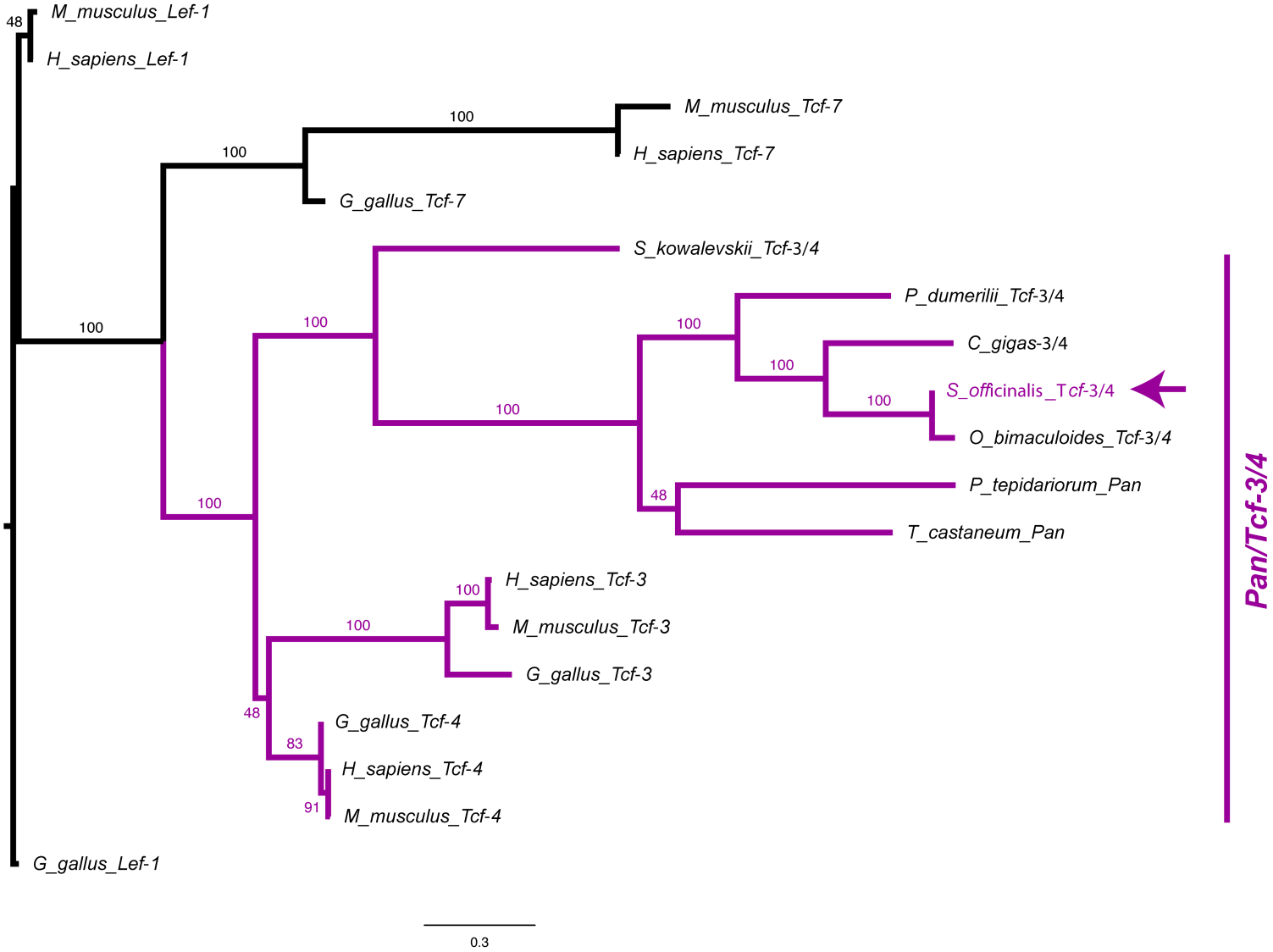

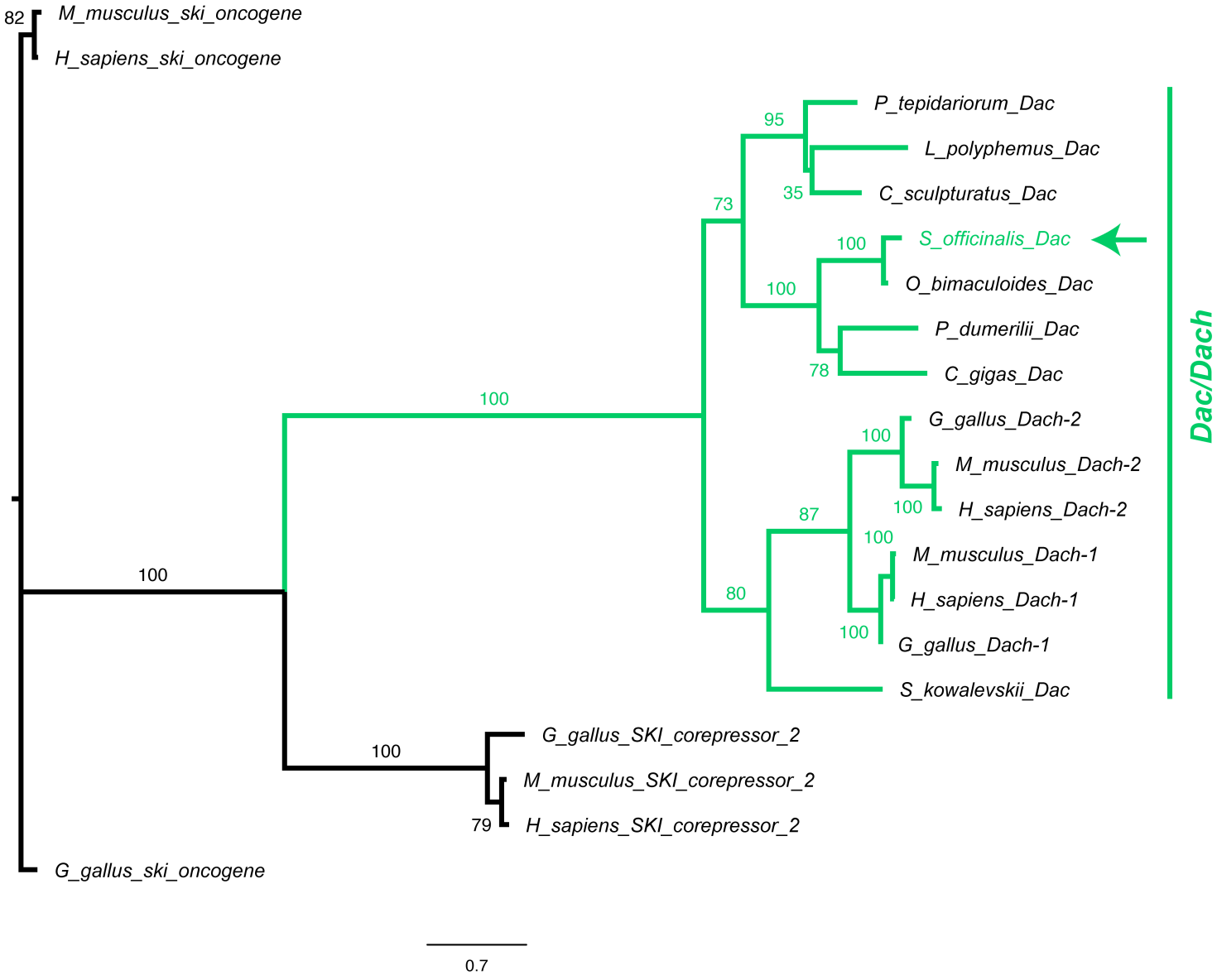

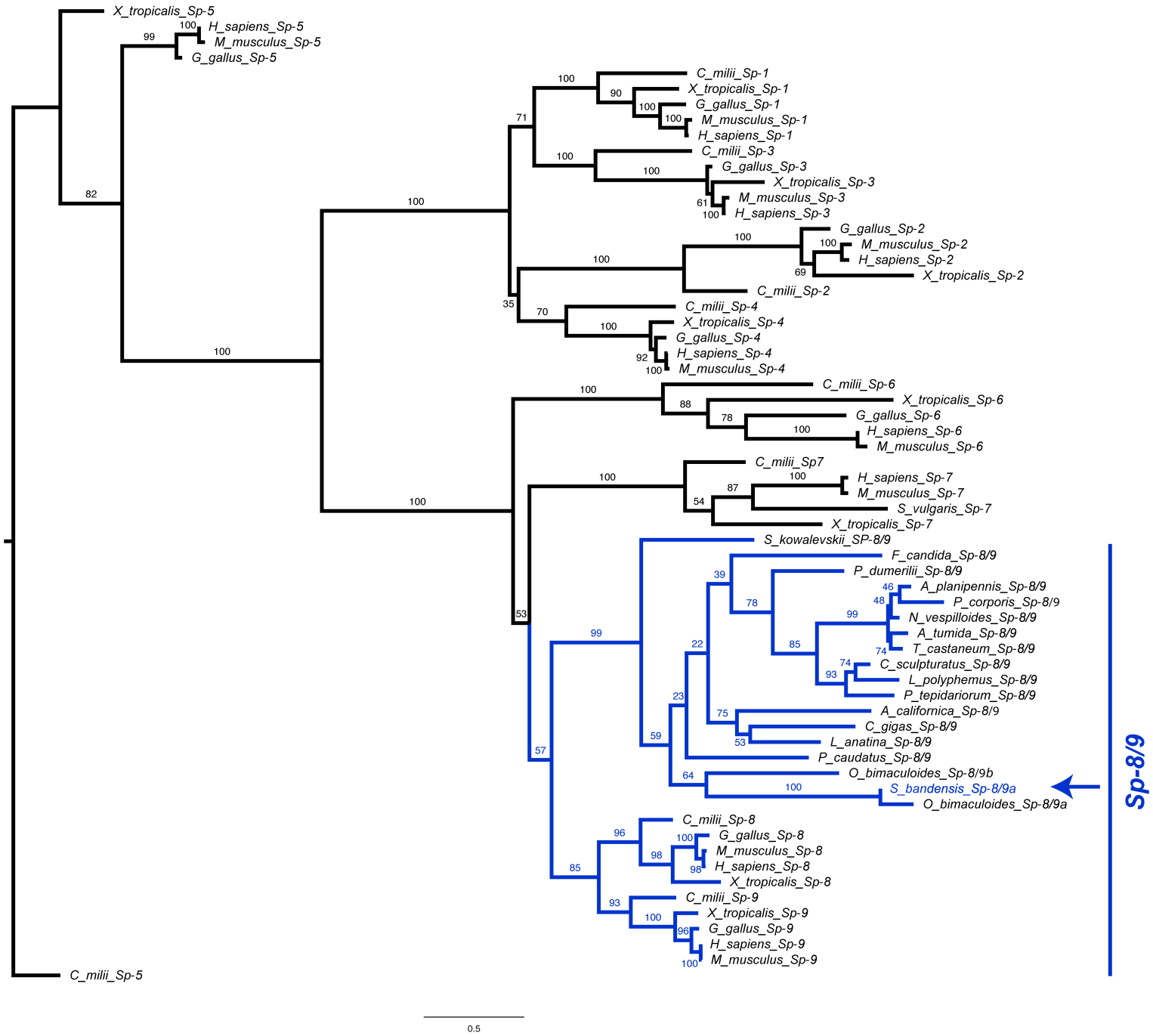

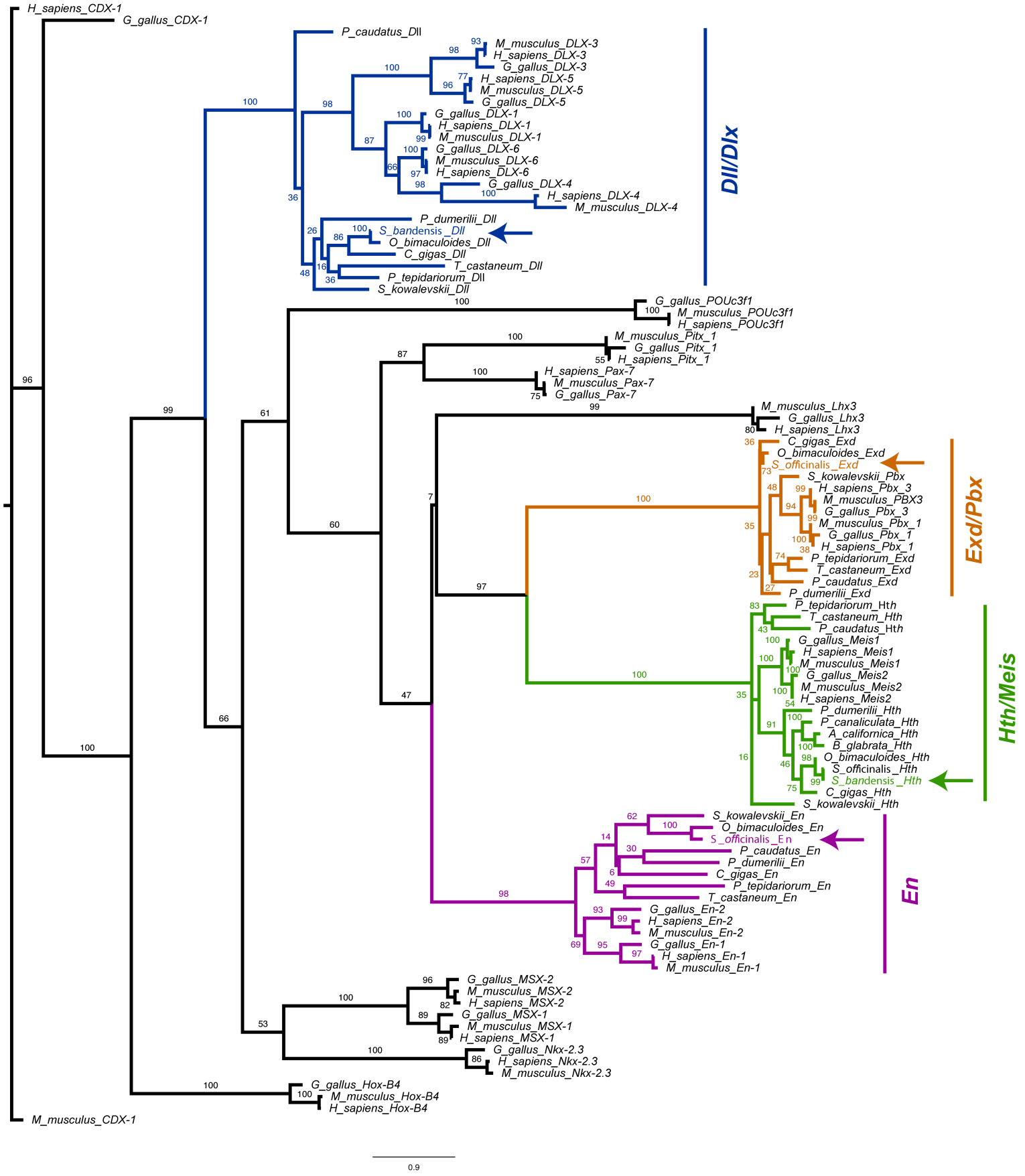

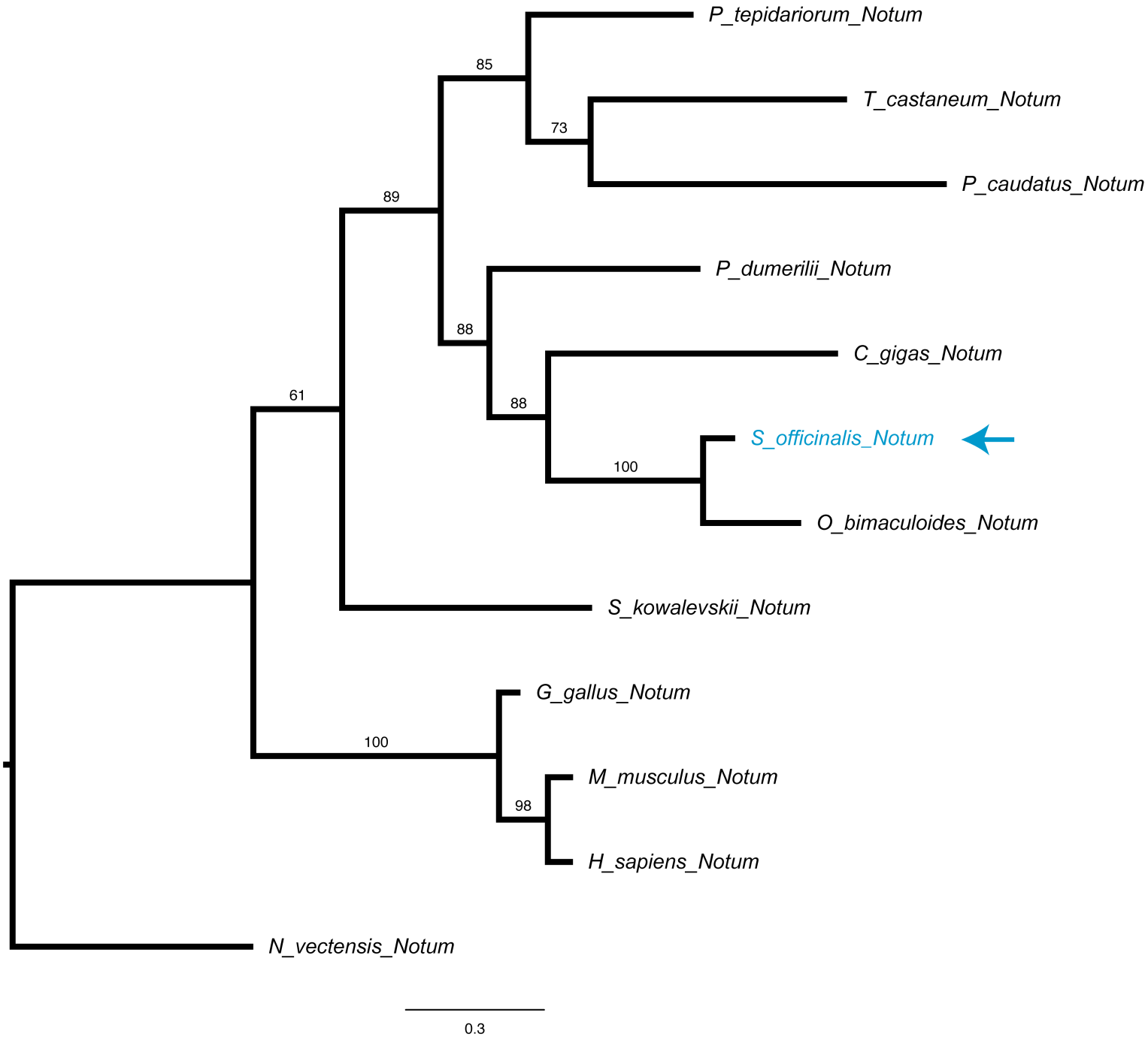

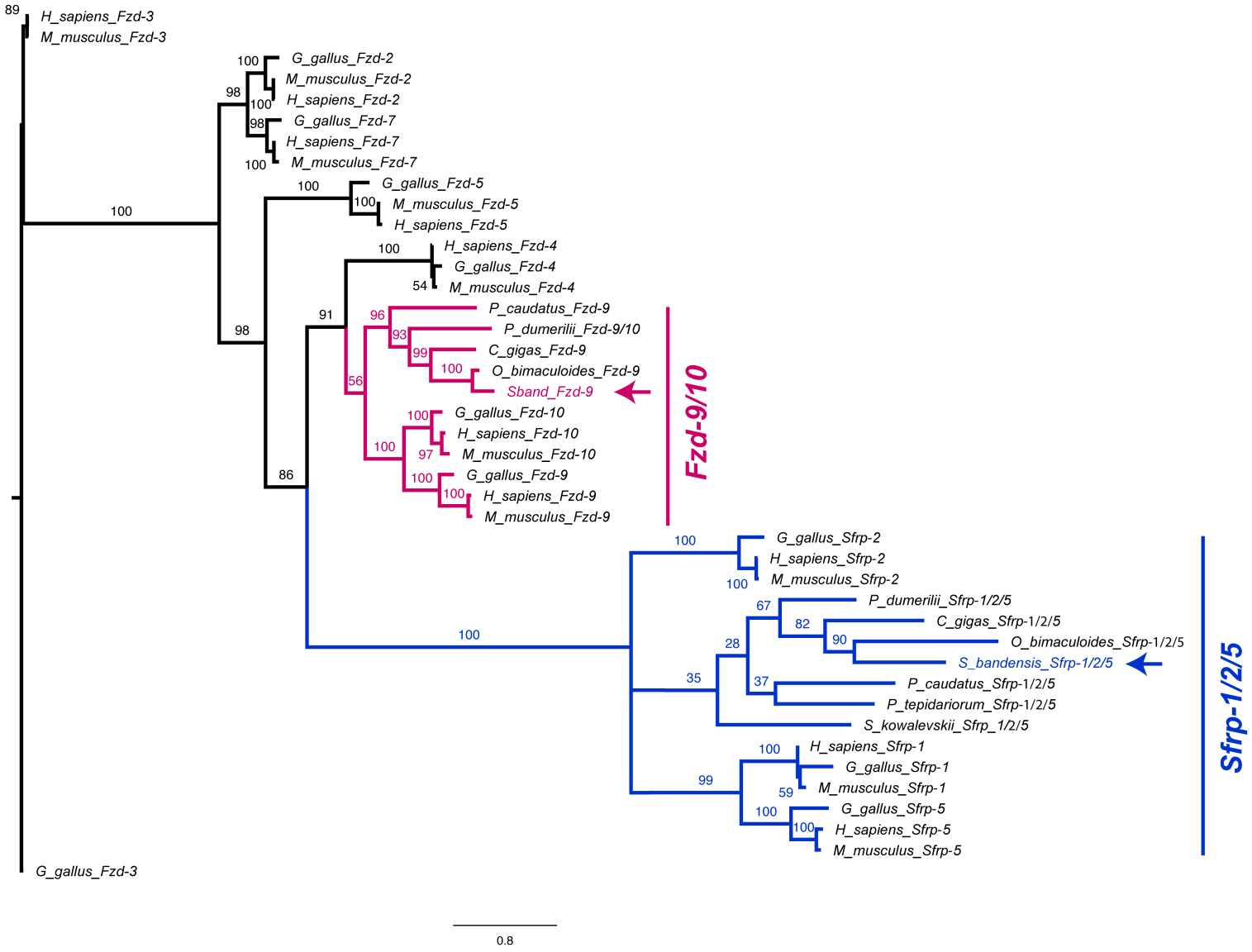

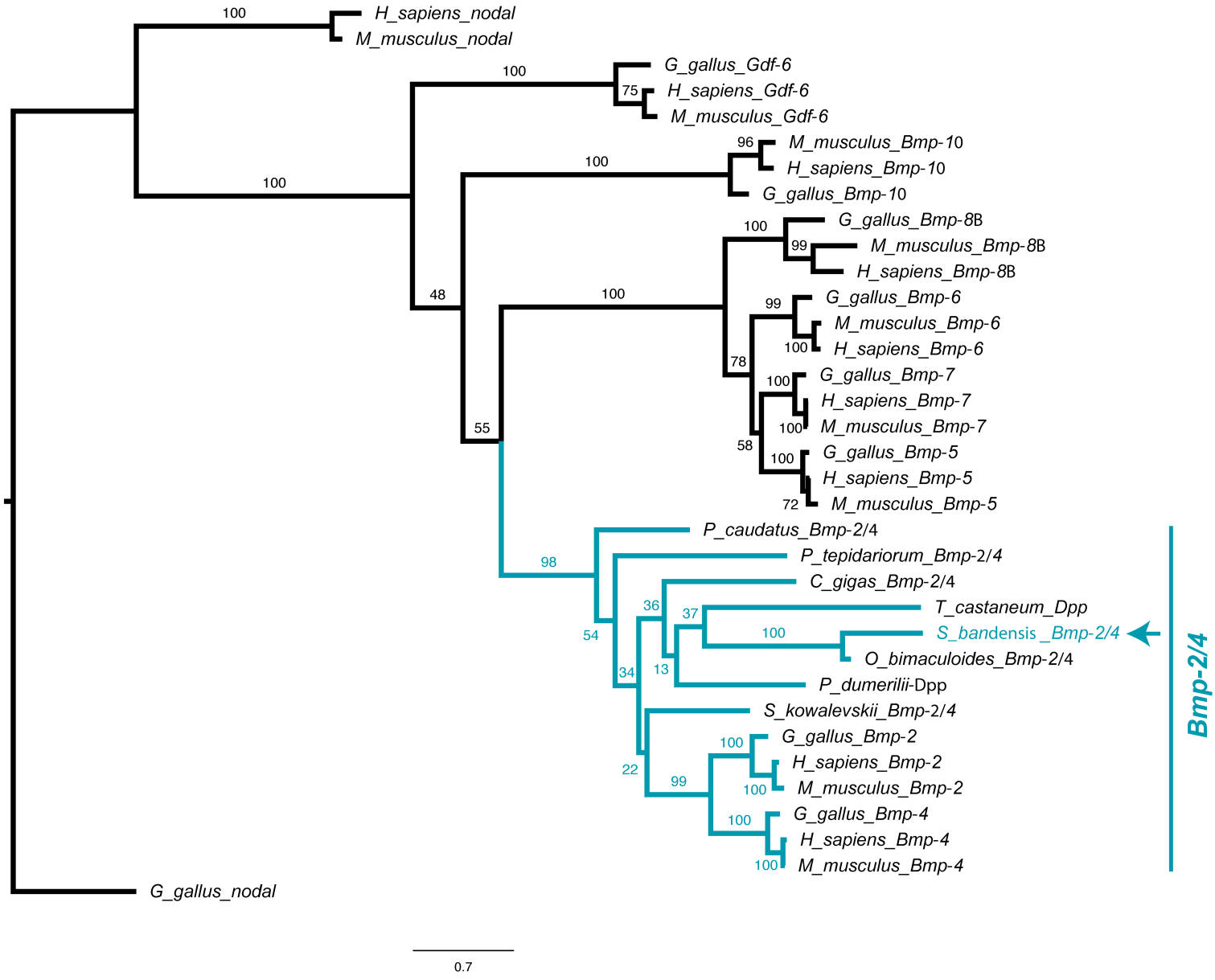

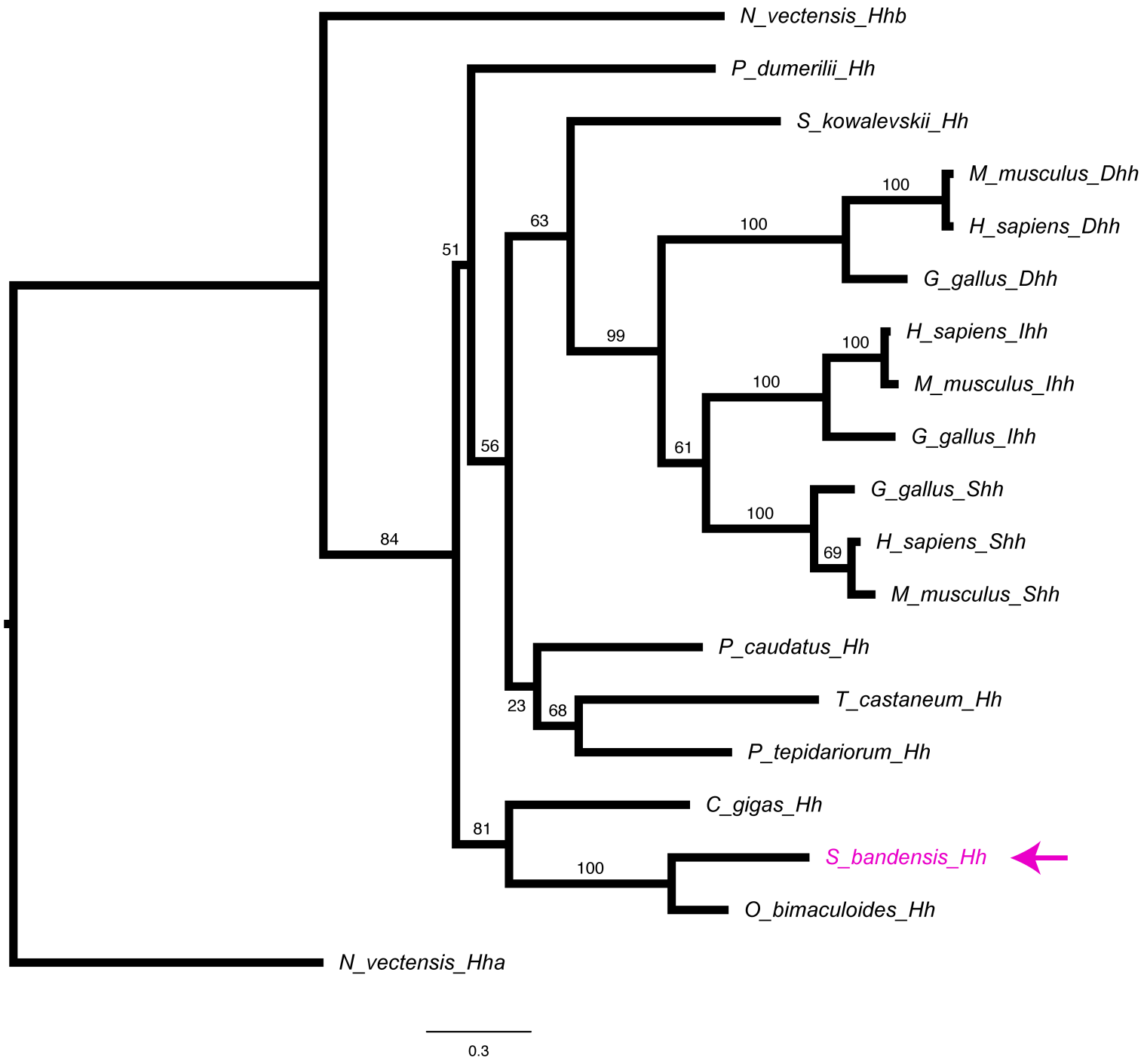

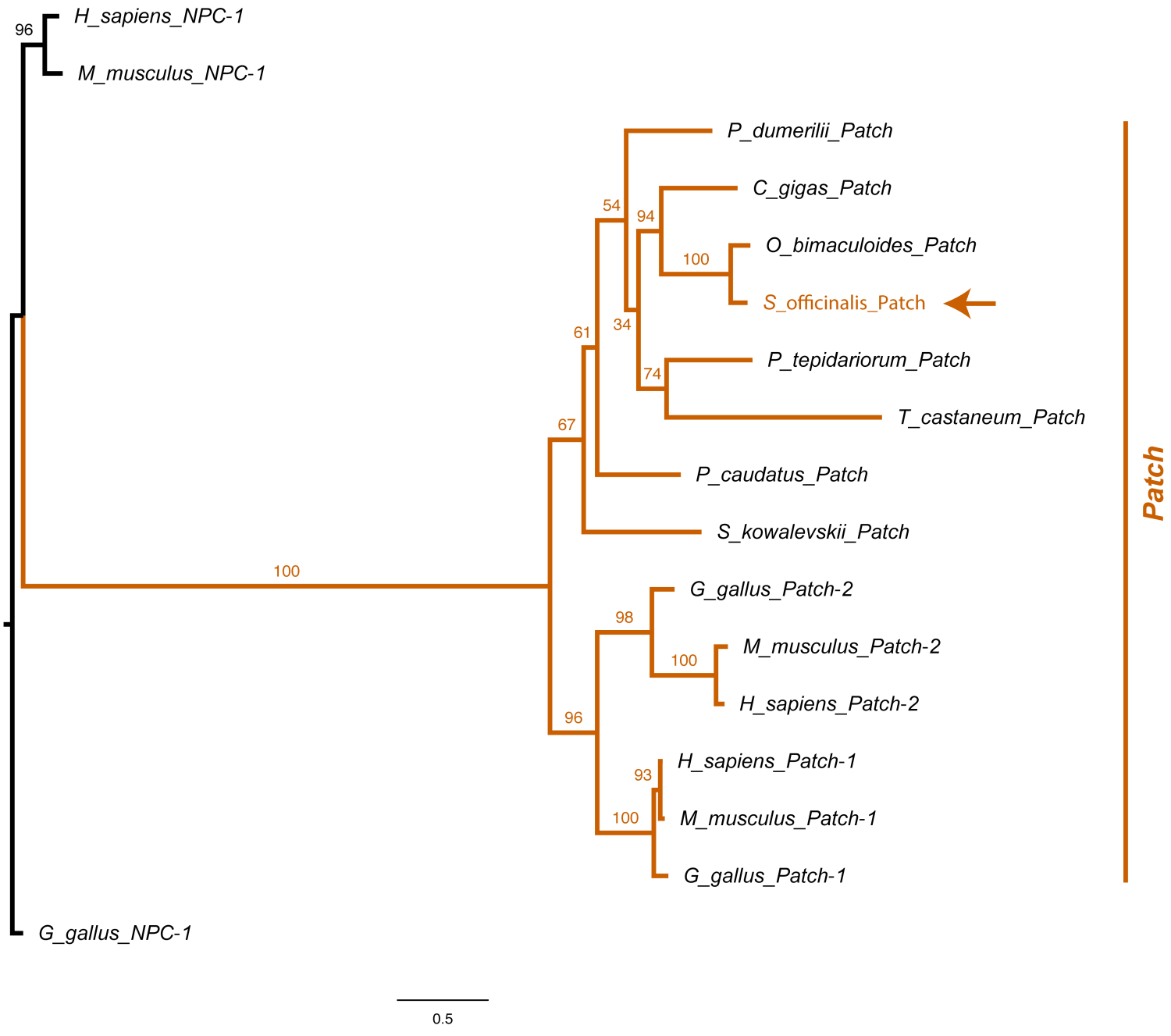

Figure 3 supplements

***Figure 3 – figure supplement 1*. Expression of developmental control genes in cuttlefish limb buds.** (**A** to **O**) *In situ* hybridizations showing *Wnt1*, *Wnt5*, *Wnt7*, *Tcf*, *Exd*, *Htx*, *Dll*, *Dac*, *Sp8*, *Hh*, *Ptc*, *Bmp2*/4, *En* and *Sfrp1/2/5* in stage 21 embryos. *Hh* expression in stage 21 limb buds, detected by *in situ* hybridizations in whole mount (F) and cryosections (K) showing the central expression in the brachial nerve cell precursors. (**P** to **R**) *In situ* hybridizations of *Frz9/10* at stages 17 (P and S), 20 (Q and T) and 21(R and U). A, anterior; P, posterior; D, dorsal; V, ventral.

***Figure 3 – figure supplement 2.* Analysis of gene expression in the arms and tentacles of *Sepia bandensis* embryos**. *S. bandensis* probes that were used on *S. officinalis* embryos were validated by species-specific hybridization using *S. bandensis* embryos. Each probe yielded identical patterns of expression in the limb buds of the two *Sepia* species. **(A-C)** Stage 20 *S. bandensis* limb buds show proximodistally regionalized expression of *Htx*, *Dll* and *Sp8/9a*. The *Htx* domain (A) is proximal to the *Dll* (B) and *Sp8/9a* (C) expression domains. **(D)** *Hh* is restricted to the anterior margin of the limb bud of *S. bandensis*. **(E, F)**, Dorsal expression of *Bmp2/4* (E) and *Sfrp1/2/5* (F) in stage 20 *S. bandensis* limb buds. **(G, H)** *Wnt5* (G) and *Frz9/10* (H) are expressed in the distal but are undetectable in the proximal regions of *S. bandensis* limb buds. **(I, J)** Two-color *in situ* hybridizations show that proximally restricted expression of *Htx* (purple) and distally restricted expression of *Wnt1* (red) are retained during *S. bandensis* limb outgrowth. Stage 21 arm (I) and tentacle (J). D, dorsal; V, ventral; P, posterior; A, anterior. All limb buds oriented as in (A) except for (D), which is oriented according to the axes shown.

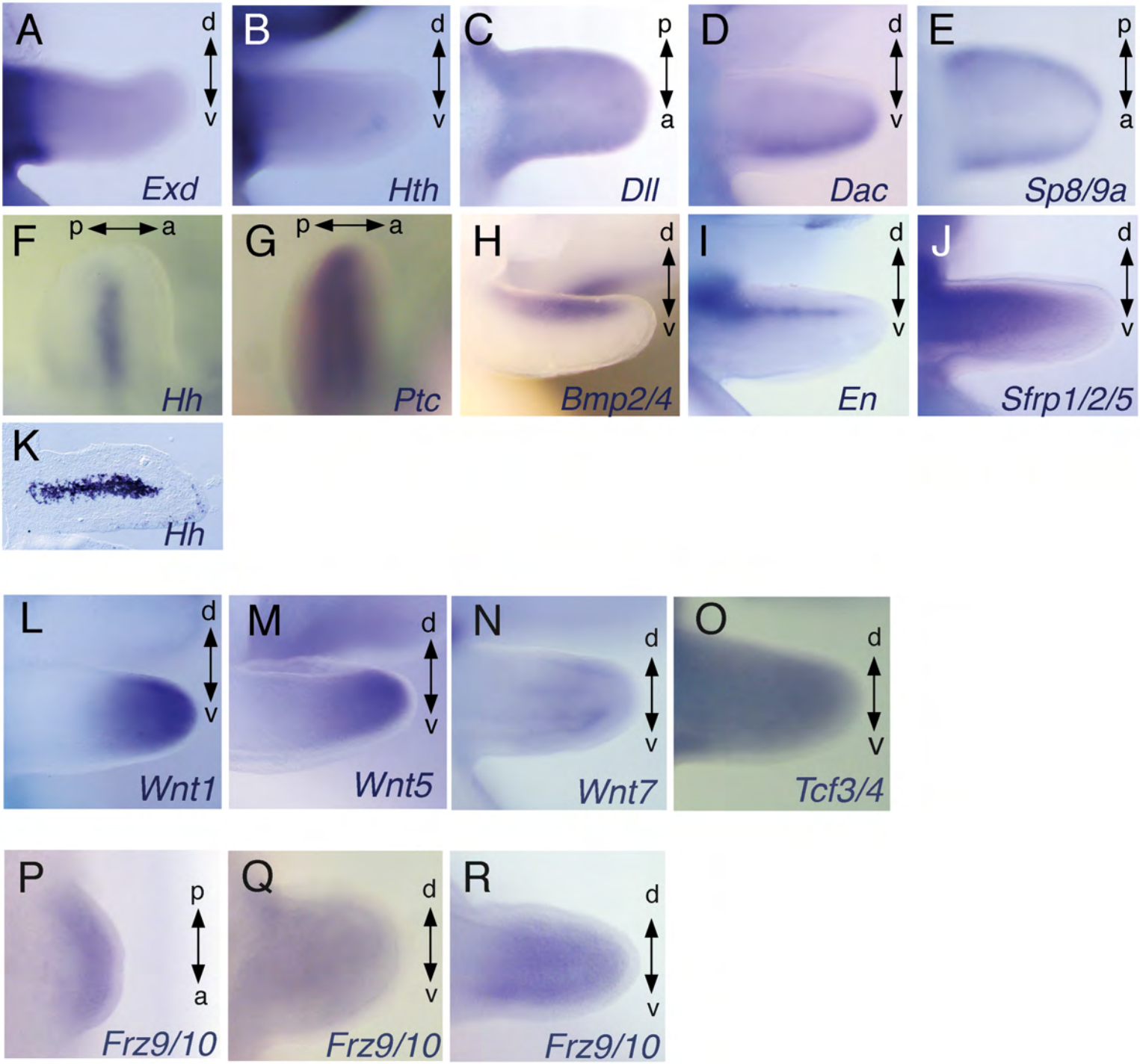

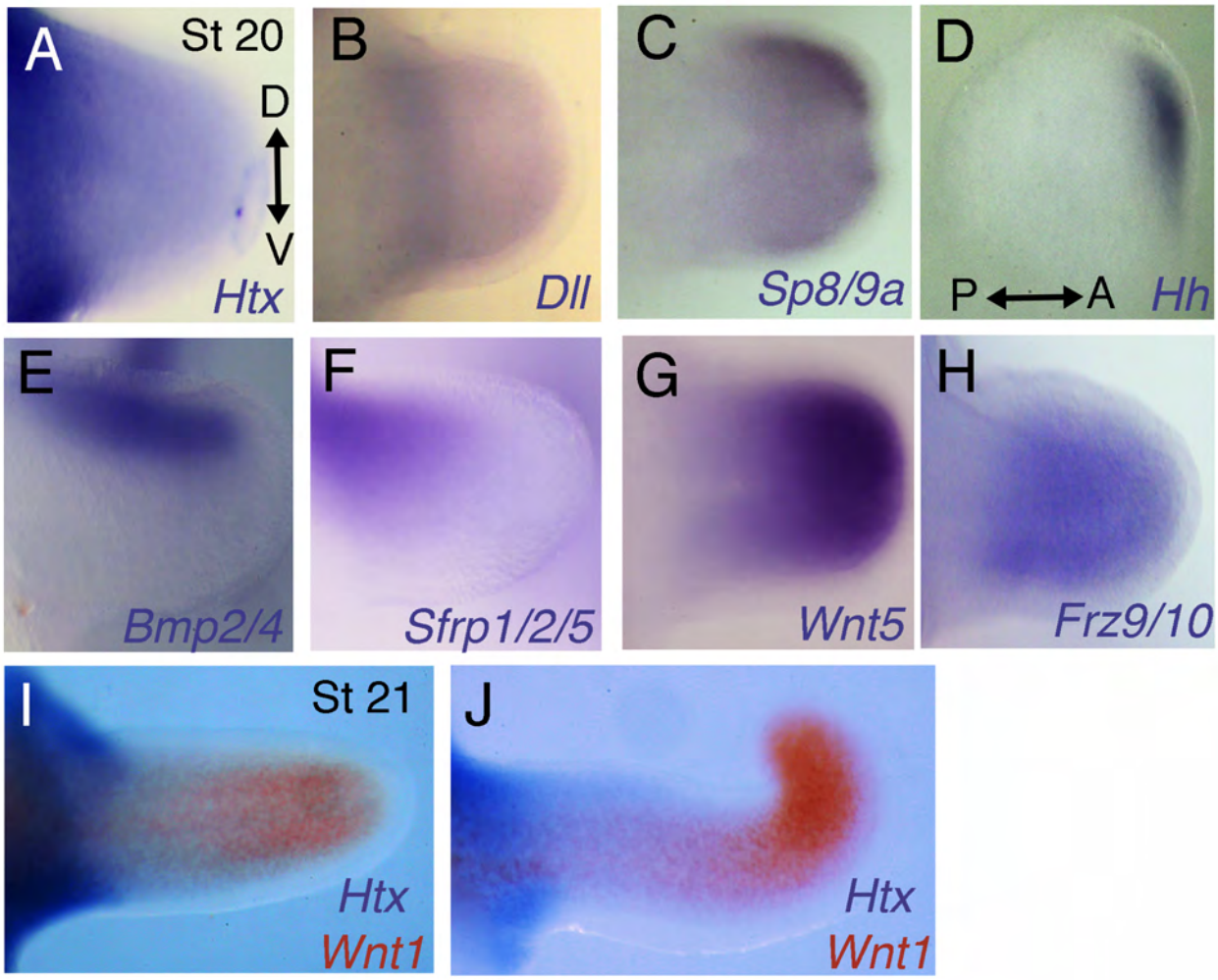

Figure 4 supplements

***Figure 4 – figure supplement 1*. Sucker development after manipulations of Bmp and Hh signaling pathways.** (**A**) SEM of Noggin-treated limbs shows dorsal ectopic sucker buds (A) as seen in Fig. 4b. (**B**) Higher magnification of the region inside the yellow square in (A) showing the superficial dome-shape morphology of sucker bud cells. (**C**) SEM of posterior mirror-image duplicated limb caused by graft of *Hh*-expressing tissue, as seen in (Fig. 4e). (**D**) Higher magnification of the region inside the yellow square in (C) shows the superficial dome-shape morphology of sucker bud cells. (**E** and **F**) Differentiation of brachial nerves in cyclopamine-treated (E) and DMSO control (F) embryos revealed by acetylated tubulin in the center of the limbs. Scale bars, 100 μm.

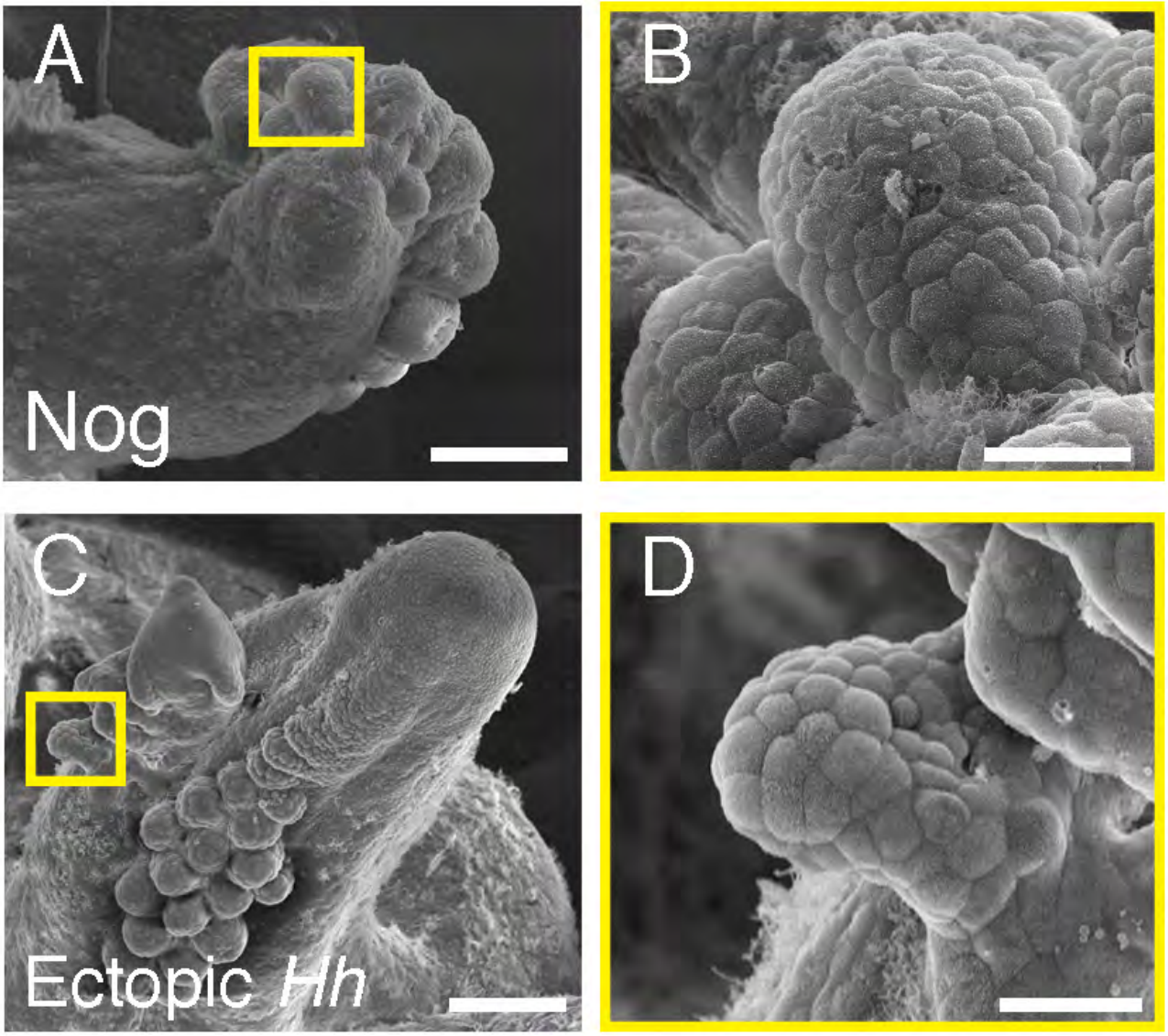

Brachial nerve differentiation

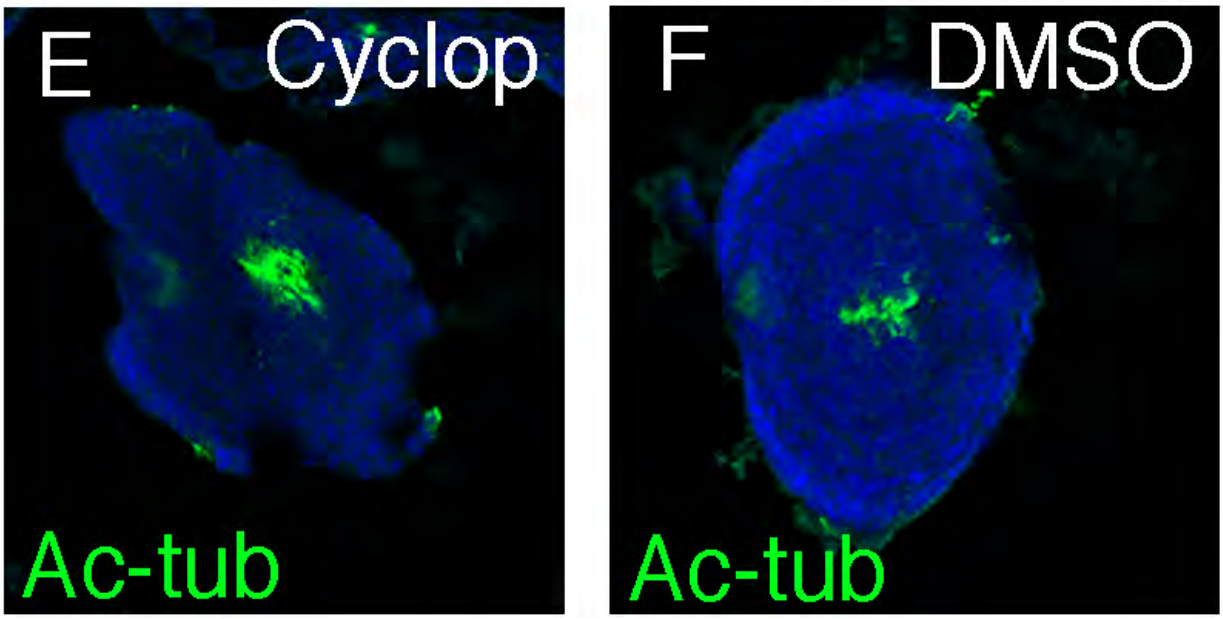

Figure 5 supplements

Figure 5 – figure supplement 1. **The developing funnel/siphon organ shows limb-like expression patterns of the proximodistal patterning genes *Exd* and *Wnt5***. (**A** to **D**) OPT reconstructions of stage 17 to 24 cuttlefish embryos showing the developing funnel/siphon system (pseudocolored red). (A) Funnel development begins at stage 17 with emergence of two bilaterally symmetrical funnel ridges between the row limb buds (bottom) and the gill primordia (GP), which can be seen adjacent to mantle (Mnt). (B) The funnel ridges fuse medially to form the funnel primordum. Yellow box marks area shown in E and F. (C) A single siphon tube then develops at the distal end of the funnel primordium. (D) By stage 24, the funnel/siphon organ has reached a miniature version of its adult shape and form. At this stage, the mantle covers the proximal region of the funnel. To allow the entire funnel/siphon organ to be seen, we segmented out the funnel and digitally removed part of the mantle using Amira Software. (**E-H**) Whole mount *in situ* hybridizations show polarized expression of *Wnt5* and *Exd* in the distal and proximal regions, respectively, of the developing funnel primordium. OPT reconstructions (E, F) and brightfield microscopy (E, G). *Wnt5* is expressed distally (arrows) at early and late stages of funnel/siphon development. In addition to the distal medial domain of *Wnt5* expression domain at stage 19+ (white arrow in E), two lateral spots of expression can be seen (white arrowheads in E). (F, H) *Exd* is expressed proximally (arrows) at both stages. Asterisks mark expression of *Exd* in the proximal ends of the funnel that are situated beneath the mantle.